PSYCHOLOGICAL SCIENCE

Measuring utility with diffusion models

Renato Berlinghieri[1]†, Ian Krajbich[2,3,4]†*, Fabio Maccheroni[5]†, Massimo Marinacci[5]†, Marco Pirazzini[6]†

The drift diffusion model (DDM) is a prominent account of how people make decisions. Many of these decisions involve comparing two alternatives based on differences of perceived stimulus magnitudes, such as economic values. Here, we propose a consistent estimator for the parameters of a DDM in such cases. This estimator allows us to derive decision thresholds, drift rates, and subjective percepts (i.e., utilities in economic choice) directly from the experimental data. This eliminates the need to measure these values separately or to assume specific functional forms for them. Our method also allows one to predict drift rates for comparisons that did not occur in the dataset. We apply the method to two datasets, one comparing probabilities of earning a fixed reward and one comparing objects of variable reward value. Our analysis indicates that both datasets conform well to the DDM. We find that utilities are linear in probability and slightly convex in reward.

INTRODUCTION

There is a growing consensus that many decisions are made using a process where decision-makers accumulate noisy evidence about the options until the net evidence exceeds a predetermined threshold (*1*–*3*). This decision process is captured by the diffusion decision model (*4*), also known as the drift diffusion model (DDM). The DDM explains both choice and response time (RT) data on tasks including perceptual decisions (*5*)—e.g., recognition memory, brightness discrimination, and dot motion direction—and economic (value-based) decisions—e.g., consumer choice (*3*, *6*–*10*), risky choice (*11*–*16*), intertemporal choice (*13*, *15*, *17*, *18*), and social preferences (*15*, *19*, *20*).

The DDM provides a mapping from subjective evidence to choice probabilities and RT distributions. It is, however, agnostic about the mapping from objective characteristics of the options/stimuli to subjective evidence. This poses a problem for modelers who do not know what decision-makers perceive, only what they are shown. To get around this issue, modelers typically take one of two approaches.

The ideal approach is nonparametric (*21*). Here, modelers identify trials that they think are roughly equivalent, bin them together into different conditions, and then use the DDM to estimate the average evidence (i.e., drift rate) for each condition separately (*22*). This requires researchers to make assumptions about what should or should not affect drift rate and needs large amounts of data.

Other researchers sometimes assume functional forms of how stimulus features should affect drift rate (*3*). In economics, this amounts to imposing a particular utility function. This can be problematic as it may not be obvious what kind of function is appropriate. For example, numerosity representation can be logarithmic or linear depending on whether there is a single array or a comparison of two arrays (*23*). Ideally, one would not need to make such assumptions but rather let the data speak for itself.

In contrast to the above approaches, we propose a more fundamental take on the problem. Baldassi *et al.* (*24*) provide a way to test the hypothesis that individuals follow a DDM in which the drift rate is based on the difference of perceived stimulus magnitudes—a difference-based DDM. We build on their ideas by constructing consistent estimators for DDM parameters, which allow us to derive the subjective evidence from behavior rather than assuming it. This is a semiparametric approach in that we assume a difference-based DDM and the restrictions that come along with it, but we put no other restrictions on the drift-rate function.

With these estimators, we are able to obtain drift rates for each pair of options and test how those rates relate to the stimulus features. An added bonus of this approach is that it allows us to derive decision thresholds and subjective evidence directly from the data, rather than using computationally heavy, model-fitting procedures. Our estimator can be calculated in microseconds, rather than the hours or days that it can take to fit the DDM to a group of individuals.

We test this approach using two choice tasks taken from Cavanagh *et al.* (*25*) and Shevlin *et al.* (*26*). In both choice tasks, participants were presented with two options and asked to choose the preferred one. In the (*25*) task, every option had the same two outcomes (win or lose) but varying probabilities. In the (*26*) task, every option had different, but deterministic, cash values. In the (*25*) task, option values were retrieved from memory, while in the (*26*) task they were constructed on the spot.

We selected these two tasks because participants were trying to maximize along a single dimension (probability or reward amount) and we know the options' objective values along those dimensions. This allows us to estimate the mapping from objective stimuli to subjective evidence. While these two tasks both involve economic choice, our theory applies to any choice task where the drift rate depends on perceived differences in stimulus magnitudes of any kind. Our theory also applies to more standard economic choice with options that vary along multiple dimensions but that can be summarized using a single subjective value. While there are surely some differences between subjective- and objective-value tasks, there are also many commonalities. Both tasks have been shown

[1]Laboratory for Information and Decision Systems, Massachusetts Institute of Technology, Cambridge, MA, USA. [2]Department of Psychology, The Ohio State University, Columbus, OH, USA. [3]Department of Economics, The Ohio State University, Columbus, OH, USA. [4]Department of Psychology, University of California, Los Angeles, Los Angeles, CA, USA. [5]Department of Decision Sciences, Bocconi University, Milan, Italy. [6]Department of Computer Science, Yale University, New Haven, CT, USA.
*Corresponding author. Email: krajbich@ucla.edu
†These authors contributed equally to this work.

to recruit the reward network (*27*, *28*) and are well explained by difference-based DDMs (*29*). Also, many models in economics make no distinction between objective and subjective values.

To preview the results, we find that in both datasets, our estimates yield the expected relationships between drift rates, choice probabilities, and RTs. We find remarkably linear relationships between the estimated drift rates—i.e., the subjective evidence—and the objective features of the stimuli, namely, the differences in probabilities (Cavanagh) and in cash rewards (Shevlin). In terms of the subjective evidence for individual options, we find that they are, on average, linear in probabilities and approximately linear, but slightly convex, in reward size. Our estimator displays several advantages over existing methods for estimating utilities: It is more accurate than logistic regression, it is much faster than standard DDM-fitting methods, and it is on more solid theoretical ground than either.

RESULTS

Difference-based DDMs

Let A be a choice set consisting of at least three alternatives, with typical elements a, b, c, and d. A DDM is a model of binary comparison between pairs of alternatives a and b. According to this model, noisy evidence about alternatives is accumulated at average rate $\mu_{a,b} = -\mu_{b,a}$, known as the drift rate, until an alternative is selected when the evidence in its favor attains a posited threshold level $\lambda > 0$, called decision threshold, boundary, or barrier.

Specifically:

1. The net evidence in favor of a against b is given, at each $t > 0$, by

$$Z_{a,b}(t) = \mu_{a,b}t + \sigma B(t) \tag{1}$$

where B is a standard Brownian motion and σ is a noise coefficient [see, e.g., Oksendal (*30*)].

2. Comparison ends when the Brownian motion $Z_{a,b}$ reaches either the barrier λ or $-\lambda$; so, the decision time (DT) is the random variable

$$\mathrm{DT}_{a,b} = \min\{t : Z_{a,b}(t) = \lambda \text{ or } Z_{a,b}(t) = -\lambda\}$$

Here, we equate DT and RT, a simplifying assumption that we relax in the Supplementary Materials.

3. When comparison ends, at random time $\mathrm{DT}_{a,b}$, the agent selects a if the upper barrier λ has been reached and selects b otherwise; so, the decision rule is the random variable

$$\mathrm{DO}_{a,b} = \begin{cases} a & \text{if } Z_{a,b}(\mathrm{DT}_{a,b}) = \lambda \\ b & \text{if } Z_{a,b}(\mathrm{DT}_{a,b}) = -\lambda \end{cases}$$

As the parameters λ, μ, and σ are unique up to a common positive scalar multiple, noise can be normalized by setting $\sigma = \sqrt{2}$. Thus, a DDM is uniquely identified by two parameters λ and μ. The barrier parameter λ is a number, while the drift parameter $\mu : A \times A \to \mathbb{R}$ is an antisymmetric function that associates to each pair (a, b) of alternatives the corresponding drift rate $\mu_{a,b}$. These parameters allow us to express choice probabilities, log-odds, and mean DT by

$$P_{a,b} = \mathbb{P}[\mathrm{DO}_{a,b} = a] = \frac{1}{1 + e^{-\lambda\mu_{a,b}}} \tag{2}$$

$$\ell_{a,b} = \ln\frac{P_{a,b}}{1 - P_{a,b}} = \lambda\mu_{a,b} \tag{3}$$

$$\overline{\mathrm{DT}}_{a,b} = \mathbb{E}[\mathrm{DT}_{a,b}] = \lambda^2\varphi(\ell_{a,b}) \tag{4}$$

where $\phi(x) = x^{-1}\tanh(x/2)$ for all real numbers x.

Next, we introduce the class of DDMs that are relevant in difference-based decisions.

Definition 1. A DDM with drift parameter μ is difference-based if, and only if, there exists a function $u : A \to \mathbb{R}$, called utility, such that

$$\mu_{a,b} = u(a) - u(b) \tag{5}$$

for all a and b in A.

A difference-based DDM presupposes a transformation u of physical stimuli—with $u(a)$ being the perceived magnitude of stimulus a—such that the rate of evidence accumulation $\mu_{a,b}$ depends only on perceived magnitude differences $u(a) - u(b)$. The function u represents sensation intensities in perceptual discrimination tasks and subjective values in economic tasks. The utility terminology that we adopt reflects our original emphasis on value differences, where the difference-based DDM is known as a value-based DDM.

The next simple characterization of difference-based DDMs highlights the properties that will guide our estimation exercise. In reading it, recall that a function $f : A \times A \to \mathbb{R}$ is cyclic when it satisfies the triangle equality

$$f_{a,b} = f_{a,c} + f_{c,b} \tag{6}$$

for all alternatives a, b, and c. For an antisymmetric function $f : A \times A \to \mathbb{R}$, the function $\tilde{f} : A \times A \to \mathbb{R}$ given by

$$\tilde{f}_{a,b} = \frac{1}{|A|}\sum_{c\in A}(f_{a,c} + f_{c,b})$$

is the least-square cyclic approximation of f (see Proposition 5 of the Supplementary Materials). For instance, $\tilde{\ell}$ is the least-squares cyclic approximation of the log-odds function ℓ.

Proposition 1. For a DDM with drift parameter μ, the following conditions are equivalent:

i. the DDM is difference based;
ii. the drift parameter μ is cyclic;
iii. the log-odds function ℓ coincides with $\tilde{\ell}$;
iv. for all $a \neq b$

$$\lambda = \sqrt{\frac{1}{|A|\,(|A|-1)}\sum_{c\neq d}\frac{\overline{\mathrm{DT}}_{c,d}}{\varphi(\tilde{\ell}_{c,d})}} \quad \text{and} \quad \mu_{a,b} = \frac{\tilde{\ell}_{a,b}}{\sqrt{\frac{1}{|A|(|A|-1)}\sum_{c\neq d}\frac{\overline{\mathrm{DT}}_{c,d}}{\varphi(\tilde{\ell}_{c,d})}}} \tag{7}$$

Thus, only the drift parameters that satisfy the triangle equality (Eq. 6), i.e., cyclicity, admit a difference-based representation. The next corollary shows that the relation between drift rates and utilities is indeed explicit. When μ is cyclic, we can then retrieve u from choice probabilities and mean DT via (Eq. 7).

Corollary 2. If a DDM is difference based with drift parameter μ, then, given any d in A, the function defined by

$$u(a) = \mu_{a,d} \quad \forall a \tag{8}$$

is, up to an additive constant, the only utility u which realizes (Eq. 5) for μ.

It is important to remark that the choice of the reference alternative d in (Eq. 8) is immaterial because our result implies that a change in the reference alternative can only shift u by an additive constant.

In contrast, if a drift parameter μ is not cyclic, then there is no function $u : A \to \mathbb{R}$ such that (Eq. 5) holds. In this case, the functions defined by (Eq. 8) for different reference alternatives d might rank alternatives in different ways. Thus, they cannot be interpreted as utilities (see Example 1 in the Supplementary Materials).

Value-consistent estimators

Consider an analyst who observes agents' pairwise choices several times, say n. The available observations produce empirical mean decision times $\overline{\mathrm{DT}}^n_{a,b}$, empirical choice frequencies $P^n_{a,b}$, and empirical log-odds $\ell^n_{a,b}$, for all $a \neq b$ in A. Baldassi *et al.* (*24*) have shown that through these statistics, the analyst can test the hypothesis that data are generated by a difference-based DDM. Here, we assume that this hypothesis has not been rejected, and we consider the problem of building an estimator of the parameters of the difference-based DDM that generates the data.

Definition 2. An estimator $(\hat{\lambda}^n, \hat{\mu}^n)$ of a DDM (λ, μ) is:

• statistically consistent if, and only if, $(\hat{\lambda}^n, \hat{\mu}^n) \to (\lambda, \mu)$ almost surely as $n \to \infty$.

• value consistent if, and only if, $\hat{\mu}^n$ is cyclic for all n.

The previous analysis demonstrates that estimators that are not value consistent are not conceptually appropriate for difference-based DDMs. Specifically, when an estimator is not value consistent, it may be the case that the estimated value $\hat{\mu}^n_{a,b}$ of $\mu_{a,b}$ is different from the sum $\hat{\mu}^n_{a,c} + \hat{\mu}^n_{c,b}$ of the estimated values of $\mu_{a,\,c}$ and $\mu_{c,b}$, for some alternatives a, b, and c. However, this means that the estimated DDM$(\hat{\lambda}^n, \hat{\mu})$ is not difference based, contradicting the hypothesis that the DDM being estimated is difference based. In other words, when an estimator is value inconsistent, there is no utility that represents the estimated drifts, so it does not produce the parameters of a difference-based DDM.

For instance, starting from Eq. 3 and assuming for simplicity that the analyst knows that λ = 1, she could estimate μ by replacing (theoretical) choice probabilities with empirical choice frequencies. This idea leads to the plug-in estimator [see, e.g., Wasserman (*31*)]

$$\hat{\mu}^n_{a,b} = \ell^n_{a,b} = \ln \frac{P^n_{a,b}}{1 - P^n_{a,b}} \tag{9}$$

This estimator is statistically consistent but value inconsistent as empirical log-odds are in general not cyclic (see Example 2 in the Supplementary Materials).

To address this issue, we consider the empirical adjusted log-odds function $\tilde{\ell}^n : A \times A \to \mathbb{R}$ given by

$$\begin{aligned} \tilde{\ell}^n_{a,b} &= \frac{1}{|A|} \sum_{c \in A} (\ell^n_{a,c} + \ell^n_{c,b}) \\ &= \frac{1}{|A|} \sum_{c \in A} \left(\ln \frac{P^n_{a,c}}{1 - P^n_{a,c}} + \ln \frac{P^n_{c,b}}{1 - P^n_{c,b}} \right) \end{aligned} \tag{10}$$

for all a and b in A. This function, proposed by Baldassi *et al.* (*24*), is the least-square cyclic approximation of ℓ^n and can be computed by using empirical choice frequencies. We can then plug-in empirical mean decision times $\overline{\mathrm{DT}}^n_{a,b}$ and empirical adjusted log-odds $\tilde{\ell}^n_{a,b}$ into Eq. 7 to obtain a new plug-in estimator.

Definition 3. The cyclic estimator $(\tilde{\lambda}^n, \tilde{\mu}^n)$ of a difference-based DDM is given by

$$\begin{aligned} \tilde{\lambda} &= \sqrt{\frac{1}{|A|(|A|-1)} \sum_{c \neq d} \frac{\overline{\mathrm{DT}}^n_{c,d}}{\varphi(\tilde{\ell}^n_{c,d})}} \quad \text{and} \\ \tilde{\mu}_{a,b} &= \frac{\tilde{\ell}^n_{a,b}}{\sqrt{\frac{1}{|A|(|A|-1)} \sum_{c \neq d} \frac{\overline{\mathrm{DT}}^n_{c,d}}{\varphi(\tilde{\ell}^n_{c,d})}}} \quad \forall a \neq b \end{aligned} \tag{11}$$

The next proposition shows that this estimator has the desired properties and yields an immediate utility estimation.

Proposition 3. The cyclic estimator is both statistically and value consistent. Moreover, given any d in A, the function defined by

$$\tilde{u}^n(a) = \tilde{\mu}^n_{a,d} \quad \forall a \tag{12}$$

is, up to an additive constant, the only function that satisfies

$$\tilde{\mu}^n_{a,b} = \tilde{u}^n(a) - \tilde{u}^n(b) \quad \forall a, b$$

The resulting utility estimation builds on the theoretical foundation given by the triangle equality as well as on the joint use of empirical choice frequencies and empirical DT, as suggested by the approaches of Clithero (*8*) and Webb (*32*). Again, as observed immediately after Corollary 2, the choice of the reference alternative d in (Eq. 12) is immaterial because of the cyclicity of $\tilde{\mu}^n$.

We close with an important remark. The computation of the cyclic estimator seems to require, prima facie, a complete choice dataset in which all possible pairwise comparisons of distinct alternatives in A are observed. Yet, in the Supplementary Materials, we provide a simple iterative scheme that extends the estimator to incomplete datasets by leveraging on the premise that observations are generated by an underlying difference-based DDM and an estimator for such a DDM must satisfy the triangle equality (Eq. 6).

Empirical analysis

In this section, we complete the analysis of the cyclic estimator by applying it to behavioral data from two independent experiments, one with comparisons between all pairs of options (complete) and the other with missing comparisons (incomplete). In both cases, we obtain very good fits and a "surprise." The surprise is that the utilities that we estimate mostly conform with those predicted by the most basic decision theoretic model of (expected) payoff

maximization. The goodness of fit confirms the efficiency of estimating rather than postulating the drift parameters.

Datasets

The first dataset comes from Cavanagh *et al.* (*25*) and is complete. In this study, participants chose between all pairs of six alternatives, eight times each, for a total of 120 trials per session. The alternatives were represented by Hiragana characters, each with a different probability (0.2, 0.3, 0.4, 0.6, 0.7, and 0.8) of yielding a constant reward. These probabilities were a priori unknown to the participants but learned through experience in a prior training phase. Participants completed two sessions, each with a different set of six characters.

The second dataset comes from Shevlin *et al.* (*26*) and is incomplete. In this study, participants chose between hundreds of unique alternatives. Each alternative was a 3 × 2 array of colored squares, with each color worth a different amount of money. There were 12 possible colors, each one worth a different amount of money; the values increased linearly across the color spectrum. The value of each array was the sum of the values of its six colored squares; this resulted in 27 possible array values. These arrays were divided into three value tiers: low, medium, and high value. In each trial, participants chose between two alternatives in the same tier. Like the Cavanagh *et al.* (*25*) study, the rewards for each color were a priori unknown to the participants but learned in a prior training phase. Before exclusions [as implemented by Shevlin *et al.* (*26*)], there were 135 trials per participant in the data we analyzed, or 45 trials per tier.

Both studies consisted of two parts: a training phase where the participants learned either the probabilities (Cavanagh) or the rewards (Shevlin) and a test phase where they chose from pairwise combinations of the alternatives. Training stopped when there was sufficient discrimination between correct and incorrect choices. In the test phase, participants chose between pairs of alternatives without receiving any feedback, so that choice was purely based on what had previously been learned. Here, we only analyze the test-phase trials. See Fig. 1 for further details on the tasks in these two experiments.

In summary, we study two tasks where participants learned the value of different alternatives. We chose these datasets because they present the proof of two concepts: the cyclic estimator works for both complete and incomplete datasets and for both probabilistic and deterministic rewards. They also allow us to test how the utilities reflect the objective values.

Analysis

The cyclic estimator (Eqs. 11 and 12 and their generalizations provided in the Supplementary Materials) allows us to directly estimate the drift rates (utility differences) and boundary separation (threshold) of a DDM from observable choice and RT data. In the Supplementary Materials (figs. S3 and S4), we provide evidence that the cyclic estimator accurately recovers drift rates and boundary separations in synthetic data simulated from a DDM with typical parameters. Next, we investigate the performance of the cyclic estimator on the empirical data.

The first behavioral quantity predicted by the DDM is the choice probability for each alternative pair (psychometric function). The estimated model seems to capture the psychometric behavior of the participants from both experiments with great precision (Fig. 2).

The second behavioral quantity predicted by the model is the mean DT for each binary choice (chronometric function). Before investigating the chronometric function goodness of fit, we need to deal with a systematic bias, pointed out in the literature [see, e.g., (*25*, *26*, *33*)], that high overall-value decisions ("win-win" comparisons) are faster than predicted by the vanilla DDM. In the Cavanagh *et al.* (*25*) task, these are the three comparisons between {0.8, 0.7}, {0.8, 0.6}, and {0.7, 0.6}. In the Shevlin *et al.* (*26*) task, these are the two comparisons between the highest valued arrays within each of the three value tiers. In the plots, we highlight these higher-value trials. With this caveat, the chronometric function predicted by the estimated model fits the behavioral data from both experiments nicely, as Fig. 3 shows. In the Supplementary Materials (fig. S5), we additionally present fits of the DDM to quantiles of the RT distributions, conditional on correct and error responses.

Cavanagh *et al.* (*25*) model the DDM using the difference of reward probabilities—or, equivalently, of expected payoffs—of the alternatives as drift for the binary comparisons. Analogously, Shevlin *et al.* (*26*) model the DDM using the difference of monetary payoffs as drift. We do not make these assumptions. To compare the two approaches, in Fig. 4 we examine the relationship between the objective differences in reward probabilities/monetary payoffs that they use as drifts (Δv) and our differences in estimated utility (Δu). The data show a linear relationship between these two quantities in the Cavanagh data and a slightly convex relationship in the Shevlin data.

This linear relationship between differences in payoffs and differences in estimated utilities is perhaps the most notable empirical finding of the paper. This discovery, made possible by the introduction of the cyclic estimator, suggests that the participants in the experiment actually learned the (expected) payoffs and maximized them. This optimizing behavior was assumed as an hypothesis by Cavanagh *et al.* (*25*) and Shevlin *et al.* (*26*). Our finding thus supports their assumptions.

We derive absolute utilities from relative utilities by fixing the lowest payoff alternative as a reference (Fig. 5). In the Cavanagh *et al.* (*25*) task, the relation between utilities and true probabilities is notably linear. This is consistent with the expected utility maximization hypothesis. In the Shevlin *et al.* (*26*) task, the relation is piecewise linear, with the slope slightly but significantly increasing with objective value. This increasing slope is consistent with the findings of Shevlin *et al.* (*26*). We established this with a linear regression of the utilities on the value range (0 to 8) within each value condition interacted with the value condition (low = −1, medium = 0, high = 1). The interaction between value and condition was significantly positive [$t(23) = 3.32$, $P = 0.003$].

We can also compare the utilities from the cyclic estimator to the utilities obtained from other methods. The traditional approach is to estimate the utilities using a logistic regression on the choice data, with dummy variables for each option. A newer and more computationally involved approach is to run an analogous regression for drift rates within the DDM. This is accomplished using the software package HDDM, which is a Bayesian hierarchical method that uses group-level choice and RT data to fit the DDM (*34*). Comparing the cyclic estimator to the logistic and HDDM estimators on the empirical data, we find that there is good agreement between all three methods, but that the cyclic estimator seems to be more linear, i.e., less prone to overfitting, than the logistic estimator (Fig. 6).

Last, we also analyzed the data from individual participants in each study. As expected, there is heterogeneity in the linearity of the relation between utilities and true values, particularly in the Cavanagh *et al.* (*25*) data.

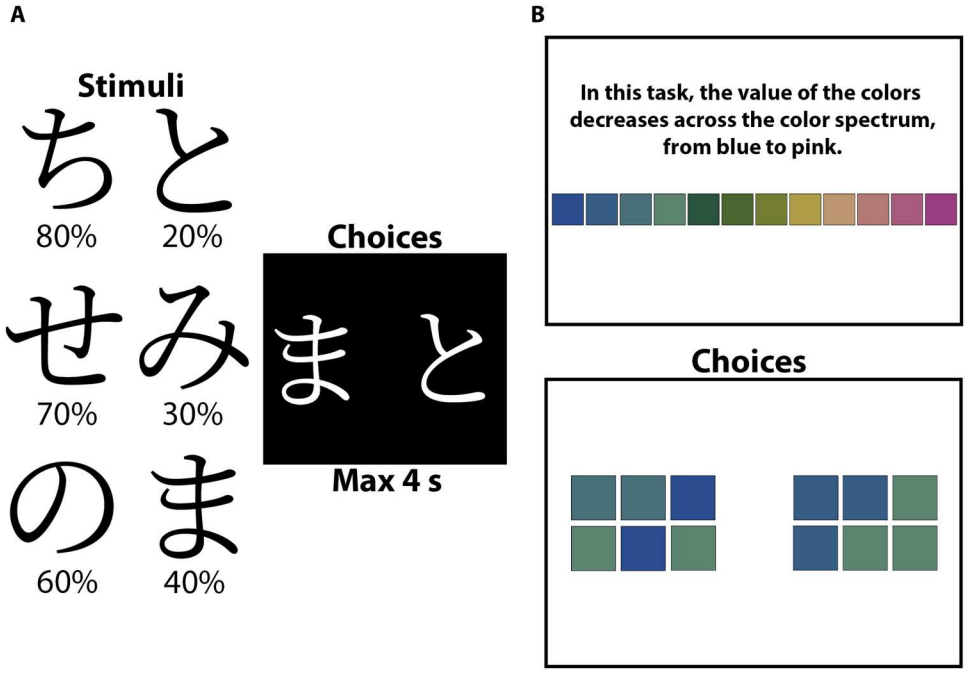

Fig. 1. Description of the experiments. (**A**) In the Cavanagh *et al.* (*25*) task, participants chose between pairs of six Hiragana characters that were trained to be associated with reward probabilities as indicated on the left. (**B**) In the Shevlin *et al.* (*26*) task, participants chose between 3 × 2 arrays of colored squares. Each color represents an integer point value from 1 to 12. The point values increased from blue to pink or pink to blue; this was counterbalanced across participants.

The individual-level analyses reveal an advantage of our cyclic estimator over other estimators like logistic regression and HDDM. If we assume that the correct estimates should be linear, then we can calculate the mean absolute error of the utility estimates for the different estimators. Our cyclic estimator has a significantly lower mean absolute error than a logistic regression estimator for the Shevlin *et al.* (*26*) dataset ($P = 10^{-10}$, $P = 10^{-12}$, $P = 10^{-13}$) though not for the Cavanagh *et al.* (*25*) dataset ($P = 0.18$). In addition, while the cyclic estimator does not outperform the HDDM estimator in mean absolute error, it uses a lot less data (single participant and choice data only) and runs in a matter of microseconds. See the Supplementary Materials (figs. S1 and S2) for more details.

DISCUSSION

Here, we used a principled approach to consistently estimate the parameters of a difference-based DDM. This allowed us to investigate how reward probabilities and amounts affect evidence accumulation (i.e., drift rates). We observed almost linear relations between differences in utilities and differences in both reward probabilities and amounts. More specifically, we observed that utilities are linear in probability and slightly convex in reward amount.

Our approach yields trial-level drift rates that show a consistent relationship with choice probabilities and RTs, as expected with the DDM. Throughout the paper, we have equated RT and DT. In reality, RT usually consists of DT as well as a non-decision time. In the Supplementary Materials (fig. S6), we show that accounting for non-decision time does indeed improve the quality of our fits. We also present an estimator that, while untested, might provide an alternative way to estimate non-decision times; we leave the validation of that estimator to future research. It is important to note that the fitting of the DDM often includes other parameters, such as starting point and across-trial variability in drift rate and starting point. Without these parameters, our estimators may suffer on datasets with substantial non-decision times, response biases, or slow/fast errors. Here, we assume that the modeler has concluded that a simple difference-based DDM is appropriate for their data. Our theory cannot be used to estimate other models or to compare them to the DDM. If the modeler wants to establish whether the DDM is appropriate for their data, then they can use the test proposed by Baldassi *et al.* (*24*).

Our method is appealing because it is free from both a priori behavioral and statistical assumptions (aside from the assumption that data are generated by a difference-based DDM) but still fits both choice probabilities and RTs well. Rather than estimating drift rates for a set of conditions, which are based on assumptions about which trials are similar, our approach estimates a unique drift rate for each comparison. Moreover, it is able to do so out-of-sample, using other comparisons in the dataset. One can even extrapolate the drift rates for comparisons not present in the data, as we did for the data of Shevlin *et al.* (*26*).

The ability to estimate drift rates for individual comparisons is a major advantage, particularly in economic choice, where drift rates depend on subjective values. Modelers typically need to measure the stimulus features in their experiments. In perceptual decisions, this is not too burdensome: typically, these features are objective and controlled by the experimenter (e.g., number, size, and brightness). In economic decisions, however, the features are often subjective and a product of the individuals' preferences. As a result, many of these experiments involve lengthy rating/evaluation tasks, in addition to the comparison tasks, to measure the subjective values of the

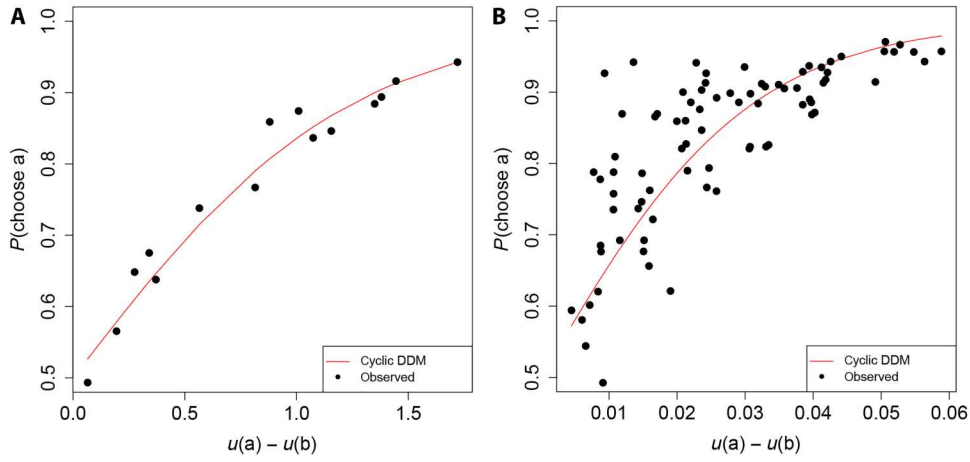

Fig. 2. Observed and estimated choice probabilities. The probability of choosing option A over option B as a function of the difference in their estimated utilities, for (**A**) the Cavanagh *et al.* (*25*) data and (**B**) the Shevlin *et al.* (*26*) data. The estimated utilities are calculated from Eqs. 10 to 12, using all comparisons {*a*, *c*} and {*c*, *b*}. The choice probabilities are either the average empirical probabilities from all direct comparisons {*a*, *b*} (black dots), or the DDM predicted probabilities calculated from Eq. 2 (red line) using the estimated parameters.

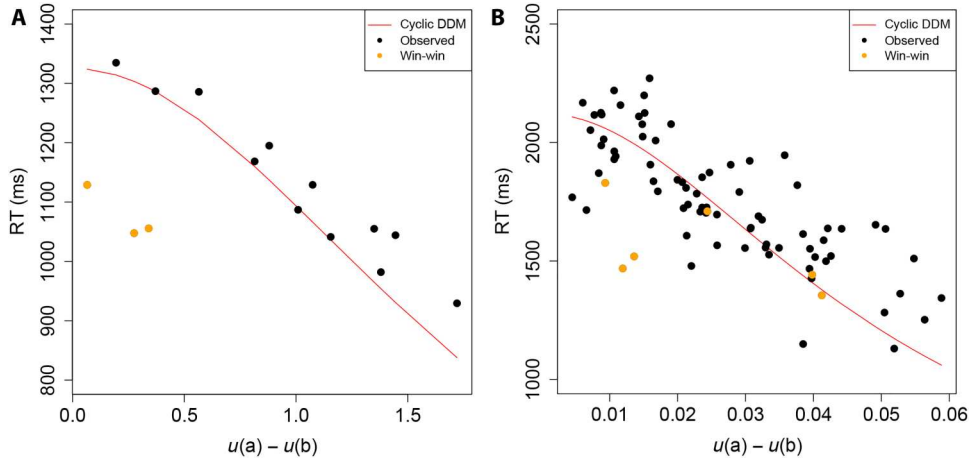

Fig. 3. Observed and estimated mean response times. The mean response time (RT; in milliseconds) in choices between option A and option B as a function of the difference in their estimated utilities, for (**A**) the Cavanagh *et al.* (*25*) data and (**B**) the Shevlin *et al.* (*26*) data. The estimated utilities are calculated from Eqs. 10 to 12, using all comparisons {*a*, *c*} and {*c*, *b*}. The RTs are either the average RT from all direct comparisons {*a*, *b*} (black dots) or the DDM predicted DT calculated from Eq. 4 (red line) using the estimated parameters. The orange dots indicate "win-win" trials, trials with the highest valued pairs of alternatives.

stimuli (*9*, *29*, *35*, *36*). Moreover, these value measurements are at odds with a "preference discovery" interpretation of the value-based DDM in which decision-makers accumulate noisy evidence about the options' subjective values that, ex ante, they only imperfectly know (*37*). By using our method, researchers might be able to avoid collecting independent evaluations of all the stimuli in their experiments. However, it is important to note that for this method to work, one must have choice probabilities (not 0 or 1) for at least some comparisons. In other words, some comparisons must be presented multiple times within an experiment, or data must be aggregated across individuals facing overlapping comparisons.

Our empirical analysis of the Cavanagh *et al.* (*25*) dataset revealed a linear function from reward probabilities to drift rates, on average. This contrasts with some of the literature on nonlinear probability weighting, where explicit probabilities are generally inverse-S weighted (overweighting of small probabilities and underweighting of large probabilities) as in prospect theory (*38*), or where learned probabilities are generally S weighted (*39*) (overweighting of large probabilities and underweighting of small probabilities). In most of this work, decision-makers face trade-offs between probability and reward size. Thus, it is possible that the linear relationship that we identified is due to the fixed rewards in the Cavanagh *et al.* (*25*) task (or perhaps the extensive training). It is also worth noting that the functions were typically not linear at the individual level (see the Supplementary Materials, fig. S1). This is consistent with the literature using this task (*40*).

Our findings are also consistent with the previous findings in the work of Shevlin *et al.* (*26*): The slightly convex utility function is consistent with their findings that drift rates are higher at higher values. At the same time, when focusing within a value level (low,

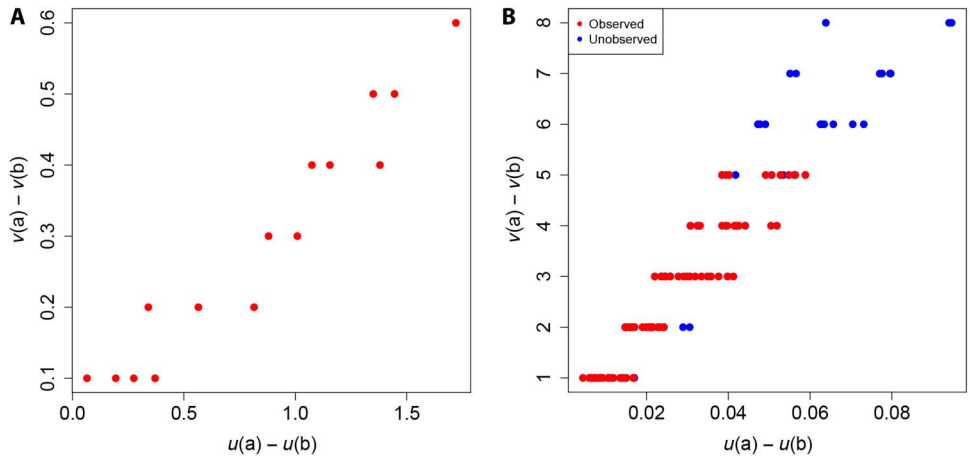

Fig. 4. Differences in objective value and estimated utility. The difference in objective value (*v*) as a function of the difference in estimated value (*u*) for each pair of options in (**A**) the Cavanagh *et al.* (*25*) data and (**B**) the Shevlin *et al.* (*26*) data. The estimated utilities are calculated from Eqs. 10 to 12, using all comparisons {*a*, *c*} and {*c*, *b*}. The objective values are the probabilities of reward in the Cavanagh *et al.* (*25*) task and the point values in the Shevlin *et al.* (*26*) task. This figure contains additional points (in blue) for comparisons {*a*, *b*} that were not in the experiment, but for which we could still estimate Δ*u* had they occurred, based on other comparisons.

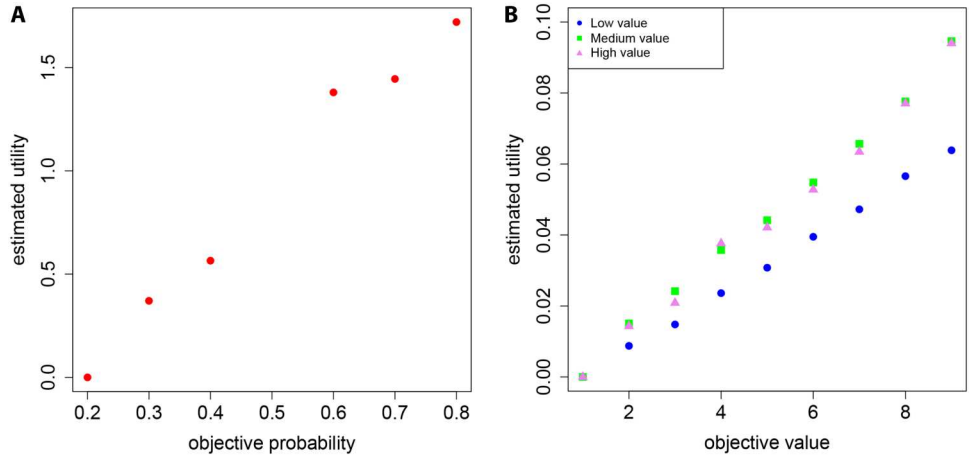

Fig. 5. Estimated utility functions. Utility vs. probability for (**A**) the Cavanagh *et al.* (*25*) data vs. (**B**) the Shevlin *et al.* (*26*) data. Analogous to Fig. 4, the estimated utilities are calculated from Eqs. 10 to 12, using all comparisons {*a*, *c*} and {*c*, *b*}, while the objective values are the probabilities of reward in the Cavanagh *et al.* (*25*) task and the point values in the Shevlin *et al.* (*26*) task. In the Shevlin *et al.* (*26*) task, we plot the data for the three different value tiers separately. Because utilities are on an arbitrary scale, we fix the lowest utility within each set to zero.

medium, or high), we find a quite linear function from objective value differences to drift rate.

There is one notable way in which the data deviate from our estimated DDM. Comparisons between the highest-value alternatives are systematically faster than expected. This is a well-documented phenomenon (*25*, *41*, *42*). There are several explanations for this phenomenon, including increased dopamine activity for high-value options and greater drift-rate variability due to attentional shifts between high-value options (*42*, *43*). These are deviations from the standard "vanilla" DDM that affect RT more than choice probabilities (see the Supplementary Materials, fig. S11). For this reason, they are highlighted only in the figures concerning RT, where they are labeled as "win-win comparisons."

Our empirical tests of the cyclic estimator were limited to objective-value tasks where options differ along a single stimulus dimension, namely, reward size and probability. We do not believe that this limits our contribution, as the conditions apply to any difference-based DDM, and we know that difference-based DDMs work well in subjective-value tasks as well. The reason that we chose to focus on objective-value tasks is because there is a ground truth that we can compare our utility estimates to. In subjective-value tasks, there is no ground truth. If we found non-linear relations between estimated and reported utilities, then we would not know whether that was an issue with the estimator or with the reports. So, while we advocate for using our estimator to infer utilities in subjective-value tasks, we did not think it was appropriate to use these tasks to validate the estimator in this article. That is a next step.

The use of DDM and other sequential sampling models has a long history in statistics (*44*) and cognitive psychology (*4*). There is also a growing literature applying such models to economic choice, most notably with decision field theory (*14*). Recent work in economics has explored the optimality of sequential sampling

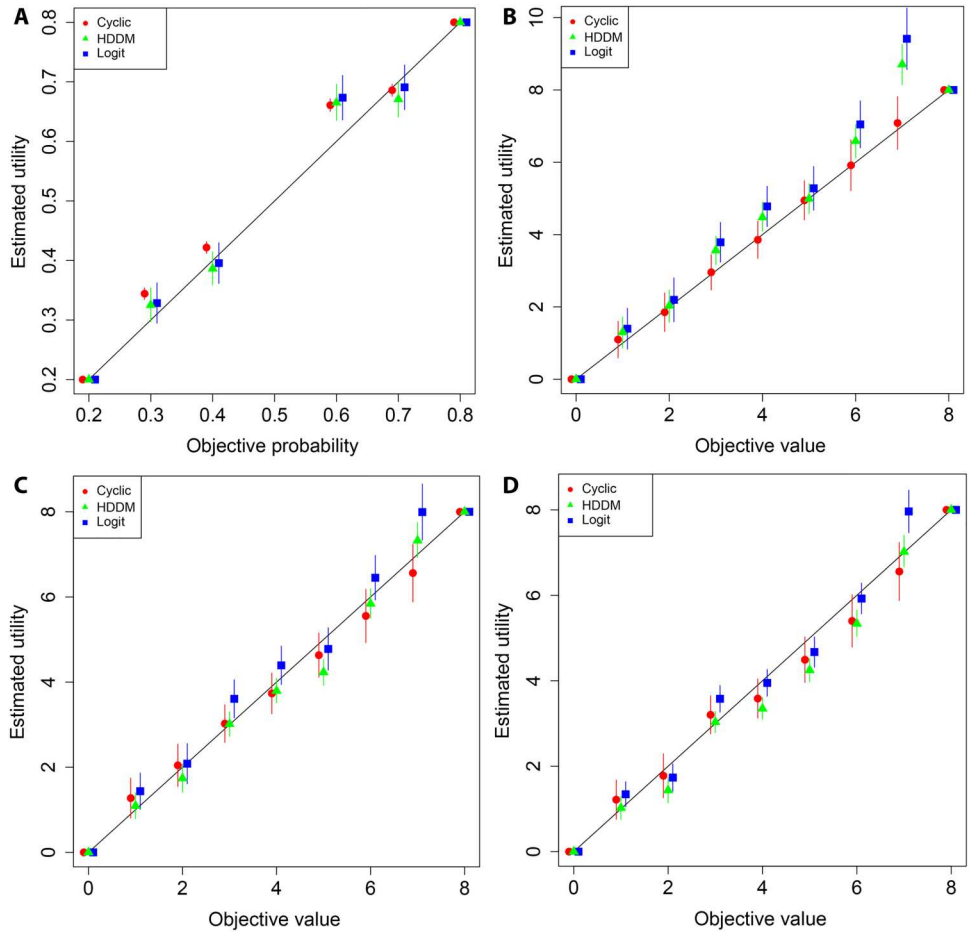

Fig. 6. Model comparison of the estimated utility functions. Utility versus probability for the (**A**) Cavanagh *et al.* (*25*) data, and versus value for the (**B** to **D**) Shevlin *et al.* (*26*) data in low-, medium-, and high-value conditions respectively. These plots display a linear relationship (diagonal black line) as well as the fits from our cyclic estimator, HDDM, and a logistic regression. Because utility is on an arbitrary scale, we forced the lowest and highest utilities to be on the diagonal and then measured the relative locations of the remaining estimates. For the logit and cyclic estimators, the bars are 95% confidence intervals; for the HDDM, the bars are 95% highest density intervals.

models and their link to strength of preference (*8*, *15*, *37*, *45*–*50*). One advantage of the DDM is that it jointly predicts choice probabilities and RT. Thus, the analysts' access to RT data should improve their ability to infer preferences or beliefs (*8*, *15*, *32*, *46*, *49*, *51*, *52*), as we also observed here with the HDDM estimator. The DDM can also be used to decompose the decision process into evaluations of the alternatives, prior biases, speed-accuracy motivation, and so on (*53*, *54*). In more recent years, these models have become very popular in cognitive neuroscience and in decision neuroscience (*1*, *55*). They can also account for eye-tracking and brain-imaging data (*3*, *20*, *35*, *56*–*60*). Our ability to estimate trial-level drift rates provides researchers with more precise inputs for modeling these data (*61*). We hope that these findings fuel further work on the DDM in economic choice (and beyond) and that these methods will be used to better understand the relation between objective and subjective evidence.

MATERIALS AND METHODS

Cavanagh task

The first dataset comes from Cavanagh *et al.* (*25*). The study included 20 participants (12 male, mean age of 20 years) from the Brown University community, who were rewarded with either 20 USD or extra course credit.

Participants performed the task twice using different nonoverlapping character sets. The mapping from characters to probabilities was randomized across participants. The data were combined across the two sessions.

Each session began with a training phase in which the probabilities were learned through reinforcement. During the training phase, participants were presented with one of three stimulus pairs with the following reinforcement probabilities 0.8/0.2, 0.7/0.3, or 0.6/0.4. Participants went through one to six blocks of training (60 stimuli each) until they made the correct choice on 0.65, 0.6, and 0.5 of the trials in the 0.8/0.2, 0.7/0.3, and 0.6/0.4 pairs, respectively. Participants who did not satisfy all these requirements by the sixth block proceeded to the test phase regardless.

In the test phase, participants chose between all pairs of six alternatives, eight times each, for a total of 120 trials per session, or

240 trials total. Trials began with a fixation cross for 1000 ms. Stimuli were presented for a maximum of 4000 ms, and disappeared as soon as a choice was made. Participants then saw a blank black screen for 1000 ms. There was no feedback in the testing phase.

Shevlin task

The second dataset comes from Shevlin *et al.* (*26*). The study included 70 participants from the Ohio State University community, who were rewarded with a show-up fee of 5 USD as well as a bonus payment based on their performance (30 points per 1 USD; mean earnings: 9.81 USD).

Participants completed two phases of the study. In the first phase, participants viewed a spectrum of 12 distinct colors. Participants were told that the value of these colors was either increasing or decreasing from left to right. Participants then completed a training phase, in which they chose between two arrays, each composed of six colored squares. The values for each colored square ranged from 1 to 12. After each choice, participants saw the values of both arrays (equal to the sum of the colored squares), as well as their total earnings. Participants first completed a block of 30 trials. If they reached or surpassed 0.70 accuracy, they proceeded to phase 2; otherwise, they completed another block of 30 trials. This process was repeated until each participant achieved 0.70 accuracy or completed six training blocks.

In phase 2, participants faced 270 binary-choice trials. Trials were constructed by first creating stimulus pairs for the middle-value condition and then subtracting or adding a constant value of 4 to every square. The arrays were constructed so that the colored squares were never all the same color, but there were no other restrictions. In addition, the value difference in each trial was always between 1 and 5 points.

In the original study, there were blocks of 15 trials, some with trials all from the same tier and some with trials from different tiers (5 from each). Here, we only analyze the latter blocks as they are the most natural. In the Supplementary Materials (figs. S7 to S10), we also examine the other blocks.

To properly constrain participants' earnings, they started out with a deficit of 10,500 points. Participants who ended the study with a negative balance only received the show-up fee. Participants were informed of this deficit and the conversion rate at the beginning of the study.

Supplementary Materials

This PDF file includes:

Supplementary Text
Figs. S1 to S11
References

REFERENCES AND NOTES

1. M. N. Shadlen, D. Shohamy, Decision making and sequential sampling from memory. *Neuron* **90**, 927–939 (2016).
2. J. R. Busemeyer, S. Gluth, J. Rieskamp, B. M. Turner, Cognitive and neural bases of multi-attribute, multi-alternative, value-based decisions. *Trends Cogn. Sci.* **23**, 251–263 (2019).
3. I. Krajbich, C. Armel, A. Rangel, Visual fixations and the computation and comparison of value in simple choice. *Nat. Neurosci.* **13**, 1292–1298 (2010).
4. R. Ratcliff, A theory of memory retrieval. *Psychol. Rev.* **85**, 59–108 (1978).
5. R. Ratcliff, P. L. Smith, S. D. Brown, G. McKoon, Diffusion decision model: Current issues and history. *Trends Cogn. Sci.* **20**, 260–281 (2016).
6. M. Milosavljevic, J. Malmaud, A. Huth, C. Koch, A. Rangel, The drift diffusion model can account for the accuracy and reaction time of value-based choices under high and low time pressure. *Judgm. Decis. Mak.* **5**, 437–449 (2010).
7. G. Fisher, An attentional drift diffusion model over binary-attribute choice. *Cognition* **168**, 34–45 (2017).
8. J. A. Clithero, Improving out-of-sample predictions using response times and a model of the decision process. *J. Econ. Behav. Organ.* **148**, 344–375 (2018).
9. P. Sepulveda, M. Usher, N. Davies, A. A. Benson, P. Ortoleva, B. De Martino, Visual attention modulates the integration of goal-relevant evidence and not value. *eLife* **9**, e60705 (2020).
10. K. X. Chiong, M. Shum, R. Webb, R. Chen, Combining choice and response time data: A drift-diffusion model of mobile advertisements. *Manage. Sci.* 10.1287/mnsc.2023.4738, (2023).
11. M. Glickman, O. Sharoni, D. J. Levy, E. Niebur, V. Stuphorn, M. Usher, The formation of preference in risky choice. *PLOS Comput. Biol.* **15**, e1007201 (2019).
12. V. Zilker, T. Pachur, Nonlinear probability weighting can reflect attentional biases in sequential sampling. *Psychol. Rev.* **129**, 949–975 (2022).
13. W. J. Zhao, A. Diederich, J. S. Trueblood, S. Bhatia, Automatic biases in intertemporal choice. *Psychon. Bull. Rev.* **26**, 661–668 (2019).
14. J. R. Busemeyer, A. Diederich, Survey of decision field theory. *Math. Soc. Sci.* **43**, 345–370 (2002).
15. A. Konovalov, I. Krajbich, Revealed strength of preference: Inference from response times. *Judgm. Decis. Mak.* **14**, 381–394 (2019).
16. F. Sheng, A. Ramakrishnan, D. Seok, W. J. Zhao, S. Thelaus, P. Cen, M. L. Platt, Decomposing loss aversion from gaze allocation and pupil dilation. *Proc. Natl. Acad. Sci. U.S.A.* **117**, 11356–11363 (2020).
17. J. Dai, J. R. Busemeyer, A probabilistic, dynamic, and attribute-wise model of intertemporal choice. *J. Exp. Psychol. Gen.* **143**, 1489–1514 (2014).
18. D. R. Amasino, N. J. Sullivan, R. E. Kranton, S. A. Huettel, Amount and time exert independent influences on intertemporal choice. *Nat. Hum. Behav.* **3**, 383–392 (2019).
19. I. Krajbich, T. Hare, B. Bartling, Y. Morishima, E. Fehr, A common mechanism underlying food choice and social decisions. *PLOS Comput. Biol.* **11**, e1004371 (2015).
20. C. A. Hutcherson, B. Bushong, A. Rangel, A neurocomputational model of altruistic choice and its implications. *Neuron* **87**, 451–462 (2015).
21. M. Abdellaoui, Parameter-free elicitation of utility and probability weighting functions. *Manage. Sci.* **46**, 1497–1512 (2000).
22. R. Ratcliff, P. L. Smith, A comparison of sequential sampling models for two-choice reaction time. *Psychol. Rev.* **111**, 333–367 (2004).
23. R. Ratcliff, G. McKoon, Modeling numerosity representation with an integrated diffusion model. *Psychol. Rev.* **125**, 183–217 (2018).
24. C. Baldassi, S. Cerreia-Vioglio, F. Maccheroni, M. Marinacci, M. Pirazzini, A behavioral characterization of the drift diffusion model and its multialternative extension for choice under time pressure. *Manage. Sci.* **66**, 5075–5093 (2020).
25. J. F. Cavanagh, T. V. Wiecki, A. Kochar, M. J. Frank, Eye tracking and pupillometry are indicators of dissociable latent decision processes. *J. Exp. Psychol. Gen.* **143**, 1476–1488 (2014).
26. B. R. K. Shevlin, S. M. Smith, J. Hausfeld, I. Krajbich, High-value decisions are fast and accurate, inconsistent with diminishing value sensitivity. *Proc. Natl. Acad. Sci.* **119**, e2101508119 (2022).
27. O. Bartra, J. T. McGuire, J. W. Kable, The valuation system: A coordinate-based meta-analysis of bold fmri experiments examining neural correlates of subjective value. *Neuroimage* **76**, 412–427 (2013).
28. J. A. Clithero, A. Rangel, Informatic parcellation of the network involved in the computation of subjective value. *Soc. Cogn. Affect. Neurosci.* **9**, 1289–1302 (2014).
29. S. M. Smith, I. Krajbich, Mental representations distinguish value-based decisions from perceptual decisions. *Psychon. Bull. Rev.* **28**, 1413–1422 (2021).
30. B. Oksendal, *Stochastic Differential Equations: An Introduction with Applications* (Springer Science & Business Media, 2013).
31. L. Wasserman, *All of Nonparametric Statistics* (Springer Science & Business Media, 2006).
32. R. Webb, The (neural) dynamics of stochastic choice. *Manage. Sci.* **65**, 230–255 (2019).
33. M. J. Frank, Hold your horses: A dynamic computational role for the subthalamic nucleus in decision making. *Neural Netw.* **19**, 1120–1136 (2006).
34. T. V. Wiecki, M. J. Frank, A computational model of inhibitory control in frontal cortex and basal ganglia. *Psychol. Rev.* **120**, 329–355 (2013).
35. R. Polanía, I. Krajbich, M. Grueschow, C. C. Ruff, Neural oscillations and synchronization differentially support evidence accumulation in perceptual and value-based decision making. *Neuron* **82**, 709–720 (2014).
36. J. Hascher, N. Desai, I. Krajbich, Incentivized and non-incentivized liking ratings outperform willingness-to-pay in predicting choice. *Judgm. Decis. Mak.* **16**, 1464–1484 (2021).

37. S. Cerreia-Vioglio, F. Maccheroni, M. Marinacci, A. Rustichini, Multinomial logit processes and preference discovery: Inside and outside the black box. *Rev. Econ. Stud.* **90**, 1155–1194 (2023).
38. D. Kahneman, A. Tversky, On the interpretation of intuitive probability: A reply to jonathan cohen. *Cognition* **7**, 409–411 (1979).
39. R. Hertwig, G. Barron, E. U. Weber, I. Erev, Decisions from experience and the effect of rare events in risky choice. *Psychol. Sci.* **15**, 534–539 (2004).
40. M. J. Frank, L. C. Seeberger, R. C. O'reilly, By carrot or by stick: Cognitive reinforcement learning in parkinsonism. *Science* **306**, 1940–1943 (2004).
41. A. Pirrone, H. Azab, B. Y. Hayden, T. Stafford, J. A. R. Marshall, Evidence for the speed–value trade-off: Human and monkey decision making is magnitude sensitive. *Decision* **5**, 129–142 (2018).
42. B. R. K. Shevlin, I. Krajbich, Attention as a source of variability in decision-making: Accounting for overall-value effects with diffusion models. *J. Math. Psychol.* **105**, 102594 (2021).
43. R. Ratcliff, M. J. Frank, Reinforcement-based decision making in corticostriatal circuits: Mutual constraints by neurocomputational and diffusion models. *Neural Comput.* **24**, 1186–1229 (2012).
44. A. Wald, Sequential tests of statistical hypotheses. *Ann. Math. Stat.* **16**, 117–186 (1945).
45. M. Woodford, Stochastic choice: An optimizing neuroeconomic model. *Am. Econ. Rev.* **104**, 495–500 (2014).
46. F. Echenique, K. Saito, Response time and utility. *J. Econ. Behav. Organ.* **139**, 49–59 (2017).
47. D. Fudenberg, P. Strack, T. Strzalecki, Speed, accuracy, and the optimal timing of choices. *Am. Econ. Rev.* **108**, 3651–3684 (2018).
48. S. Tajima, J. Drugowitsch, A. Pouget, Optimal policy for value-based decision-making. *Nat. Commun.* **7**, 12400 (2016).
49. C. Alós-Ferrer, E. Fehr, N. Netzer, Time will tell: Recovering preferences when choices are noisy. *J. Political Econ.* **129**, 1828–1877 (2021).
50. R. Bhui, Testing optimal timing in value-linked decision making. *Comput. Brain Behav.* **2**, 85–94 (2019).
51. C. Frydman, G. Nave, Extrapolative beliefs in perceptual and economic decisions: Evidence of a common mechanism. *Manage. Sci.* **63**, 2340–2352 (2017).
52. C. Frydman, I. Krajbich, Using response times to infer others' private information: an application to information cascades. *Manage. Sci.* **68**, 2970–2986 (2022).
53. C. N. White, R. A. Poldrack, Decomposing bias in different types of simple decisions. *J. Exp. Psychol. Learn. Mem. Cogn.* **40**, 385–398 (2014).
54. N. Desai, I. Krajbich, Decomposing preferences into predispositions and evaluations. *J. Exp. Psychol. Gen.* **151**, 1883–1903 (2022).
55. R. Bogacz, E.-J. Wagenmakers, B. U. Forstmann, S. Nieuwenhuis, The neural basis of the speed–accuracy tradeoff. *Trends Neurosci.* **33**, 10–16 (2010).
56. U. Basten, G. Biele, H. R. Heekeren, C. J. Fiebach, How the brain integrates costs and benefits during decision making. *Proc. Natl. Acad. Sci. U.S.A.* **107**, 21767–21772 (2010).
57. T. A. Hare, W. Schultz, C. F. Camerer, J. P. O'Doherty, A. Rangel, Transformation of stimulus value signals into motor commands during simple choice. *Proc. Natl. Acad. Sci. U.S.A.* **108**, 18120–18125 (2011).
58. S. Gluth, J. Rieskamp, C. Büchel, Deciding when to decide: Time-variant sequential sampling models explain the emergence of value-based decisions in the human brain. *J. Neurosci.* **32**, 10686–10698 (2012).
59. B. M. Turner, L. Van Maanen, B. U. Forstmann, Informing cognitive abstractions through neuroimaging: The neural drift diffusion model. *Psychol. Rev.* **122**, 312–336 (2015).
60. M. A. Pisauro, E. Fouragnan, C. Retzler, M. G. Philiastides, Neural correlates of evidence accumulation during value-based decisions revealed via simultaneous EEG-fMRI. *Nat. Commun.* **8**, 15808 (2017).
61. S. Gluth, N. Meiran, Leave-one-trial-out, loto, a general approach to link single-trial parameters of cognitive models to neural data. *eLife* **8**, e42607 (2019).
62. J. Aczél, *Lectures on Functional Equations and Their Applications* (Academic Press, 1966).
63. E.-J. Wagenmakers, H. L. J. Van Der Maas, R. P. P. P. Grasman, An ez-diffusion model for response time and accuracy. *Psychon. Bull. Rev.* **14**, 3–22 (2007).
64. J. M. Cattell, The time of perception as a measure of differences in intensity. *Philos. Stud.* **19**, 63–68 (1902).

Acknowledgments: We thank M. Yoo for research assistance and J. Cavanagh, T. Wiecki, A. Kochar, and M. Frank for sharing their data. **Funding:** This study was supported by National Science Foundation awards 2148982 and 1554837, Cattell Sabbatical Fund (I.K.), and MIUR PRIN grant 2017CY2NCA (F.M.). **Author contributions:** All authors have contributed equally to this work. **Competing interests:** The authors declare that they have no competing interests. **Data and materials availability:** The datasets and code for the cyclic estimator are available on the Open Science Framework at: https://osf.io/qh6ag/. All other data needed to evaluate the conclusions in the paper are present in the manuscript and/or the Supplementary Materials.

Submitted 13 October 2022
Accepted 20 July 2023
Published 23 August 2023
10.1126/sciadv.adf1665

Science Advances
AAAS

Supplementary Materials for

Measuring utility with diffusion models

Renato Berlinghieri *et al.*

Corresponding author: Ian Krajbich, krajbich@ucla.edu

Sci. Adv. **9**, eadf1665 (2023)
DOI: 10.1126/sciadv.adf1665

This PDF file includes:

5 Supplementary material

5.1 Proofs and related analysis

The following lemma is classic (see, e.g., Theorem 1 on page 223 of Aczel [62]).

Lemma 4. *A function $f : A \times A \to \mathbb{R}$ is cyclic if, and only if, there exists $v : A \to \mathbb{R}$ such that*

$$f_{a,b} = v(a) - v(b) \qquad \forall (a,b) \in A \times A \tag{13}$$

In this case, the function v is unique up to an additive constant. Moreover, given any $d \in A$, the function

$$v_d(a) = f_{a,d} \qquad \forall a \in A$$

represents f in the sense of (13).

The proof is immediate once one notes that $f_{a,b} + f_{b,d} = f_{a,d}$ for all $a, b, d \in A$, so that

$$f_{a,b} = f_{a,d} - f_{b,d} = v_d(a) - v_d(b)$$

To see the irrelevance of the choice of d, consider another alternative c and the corresponding $v_c(a) = f_{a,c}$ for all alternatives a. The triangle equality implies $f_{a,c} + f_{c,d} = f_{a,d}$ for all a in A, and so $v_c(a) - v_d(a) = f_{a,c} - f_{a,d} = -f_{c,d}$, that is, $v_c = v_d - f_{c,d}$. In words, v_c and v_d are equal up to a constant.

On the notation side, we use the matrix expression $f_{a,b}$ instead of the usual $f(a,b)$ because our most important examples are the drift parameter $(a,b) \mapsto \mu_{a,b}$ and the log-odds function $(a,b) \mapsto \ell_{a,b}$. The same matrix perspective justifies the definition of *antisymmetry* of f by

$$f_{a,b} = -f_{b,a} \qquad \forall (a,b) \in A \times A$$

Proposition 5. *Let $f : A \times A \to \mathbb{R}$ be an antisymmetric function, the only solution of*

$$\min_{g \in \mathcal{G}} \sum_{a,b \in A} (f_{a,b} - g_{a,b})^2 \tag{14}$$

where $\mathcal{G}$ is the collection of all cyclic functions, is given by

$$\tilde{f}_{a,b} = \frac{1}{|A|} \sum_{c \in A} (f_{a,c} + f_{c,b})$$

for all $a, b \in A$.

Proof By Lemma 4,

$$\min_{g \in \mathcal{G}} \sum_{a,b \in A} (f_{a,b} - g_{a,b})^2 = \min_{v \in \mathbb{R}^A} \sum_{a,b \in A} (f_{a,b} - v_a + v_b)^2$$

Define

$$F(v) = \sum_{a,b \in A} (f_{a,b} - v_a + v_b)^2$$

and note that for all $c \in A$,

$$\begin{aligned} F'_c(v) &= \sum_{a \in A} 2(f_{a,c} - v_a + v_c) + \sum_{b \in A} -2(f_{c,b} - v_c + v_b) \\ &= \sum_{a \in A} 2(f_{a,c} - v_a + v_c) + \sum_{b \in A} 2(-f_{c,b} + v_c - v_b) \\ &= \sum_{a \in A} 2(f_{a,c} - v_a + v_c) + \sum_{b \in A} 2(f_{b,c} - v_b + v_c) \\ &= \sum_{a \in A} 4(f_{a,c} - v_a + v_c) \end{aligned}$$

Since F is convex, then v is a solution of

$$\min_{v \in \mathbb{R}^A} \sum_{a,b \in A} (f_{a,b} - v_a + v_b)^2 = \min_{v \in \mathbb{R}^A} F(v) \tag{15}$$

if and only if, for all $c \in A$,

$$\begin{aligned} \sum_{a \in A} (f_{a,c} - v_a + v_c) &= 0 \\ \sum_{a \in A} v_c &= \sum_{a \in A} (-f_{a,c}) + \sum_{a \in A} v_a \\ v_c &= \frac{1}{|A|} \sum_{a \in A} f_{c,a} + \underbrace{\frac{1}{|A|} \sum_{a \in A} v_a}_{\text{independent of } c} \end{aligned} \tag{16}$$

Claim The set of all solutions (15) is

$$\{v^\star + k : k \in \mathbb{R}\}$$

where

$$v^\star_x = \frac{1}{|A|}\sum_{y\in A} f_{x,y}$$

for all $x \in A$.

Proof Note that

$$\frac{1}{|A|}\sum_{a\in A} v^\star_a = \frac{1}{|A|}\sum_{a\in A}\frac{1}{|A|}\sum_{y\in A} f_{a,y} = 0$$

because f is antisymmetric. Therefore,

$$v^\star_c = \frac{1}{|A|}\sum_{y\in A} f_{c,y} + \frac{1}{|A|}\sum_{a\in A} v^\star_a \qquad \forall c \in A$$

and $v^\star$ satisfies (16), so it is a is a solution of (15). Moreover, if $v^\# = v^\star + k$ for some $k \in \mathbb{R}$, then

$$\frac{1}{|A|}\sum_{a\in A} v^\#_a = \frac{1}{|A|}\sum_{a\in A}(v^\star_a + k) = k + \frac{1}{|A|}\sum_{a\in A} v^\star_a = k$$

and so, for all $c \in A$,

$$v^\#_c = v^\star_c + k = \frac{1}{|A|}\sum_{y\in A} f_{c,y} + k = \frac{1}{|A|}\sum_{a\in A} f_{c,a} + \frac{1}{|A|}\sum_{a\in A} v^\#_a$$

and $v^\#$ satisfies (16), so it is a is a solution of (15).

Conversely, if $v^\#$ is a solution of (15), then $v^\#$ satisfies (16), that is,

$$v^\#_c = \underbrace{\frac{1}{|A|}\sum_{a\in A} f_{c,a}}_{v^\star_c} + \underbrace{\frac{1}{|A|}\sum_{a\in A} v^\#_a}_{\text{constant}} \qquad \forall c \in A$$

and so $v^\# \in \{v^\star + k : k \in \mathbb{R}\}$. □

With this, if g^* is a solution of (14), then fixing $d \in A$ and setting

$$v^*_a = g^*_{a,d} \qquad \forall a, b \in A$$

it follows that

$$g^*_{a,b} = v^*_a - v^*_b \qquad \forall a, b \in A$$

and

$$\sum_{a,b\in A}(f_{a,b} - v^*_a + v^*_b)^2 \le \sum_{a,b\in A}(f_{a,b} - v_a + v_b)^2 \qquad \forall v \in \mathbb{R}^A$$

Therefore, v^* is a solution of (15), and so $v^* = v^\star + k$ for some k in $\mathbb{R}$. It follows that

$$\begin{aligned} g^*_{a,b} &= v^*_a - v^*_b = v^\star_a - v^\star_b \\ &= \frac{1}{|A|}\sum_{y\in A} f_{a,y} - \frac{1}{|A|}\sum_{y\in A} f_{b,y} \\ &= \frac{1}{|A|}\sum_{y\in A}(f_{a,y} + f_{y,b}) = \tilde{f}_{a,b} \end{aligned}$$

for all $a, b \in A$.

Conversely, the previous computations show that

$$\tilde{f}_{a,b} = \frac{1}{|A|}\sum_{y\in A}(f_{a,y} + f_{y,b}) = v^\star_a - v^\star_b$$

for all $a, b \in A$. But then

$$\sum_{a,b\in A}\left(f_{a,b} - \tilde{f}_{a,b}\right)^2 = \sum_{a,b\in A}(f_{a,b} - v^\star_a + v^\star_b)^2 \le \sum_{a,b\in A}(f_{a,b} - v_a + v_b)^2 \qquad \forall v \in \mathbb{R}^A$$

and $\tilde{f}_{a,b}$ is a solution of (14). ■

Proof of Proposition 1 (i) implies (ii) is obvious.

(ii) implies (iii). For all $a, b \in A$,

$$\tilde{\ell}_{a,b} = \frac{1}{|A|}\sum_{c\in A}\left(\ell_{a,c}+\ell_{c,b}\right) = \frac{1}{|A|}\sum_{c\in A}\left(\lambda\mu_{a,c}+\lambda\mu_{c,b}\right) = \frac{1}{|A|}\sum_{c\in A}\lambda\mu_{a,b} = \lambda\mu_{a,b} = \ell_{a,b}$$

as wanted.

(iii) implies (iv). By (iii) and (4),

$$\frac{1}{|A|(|A|-1)}\sum_{c\neq d}\frac{\overline{\mathrm{DT}}_{c,d}}{\varphi\left(\tilde{\ell}_{c,d}\right)} = \frac{1}{|A|(|A|-1)}\sum_{c\neq d}\frac{\overline{\mathrm{DT}}_{c,d}}{\varphi\left(\ell_{c,d}\right)} = \frac{1}{|A|(|A|-1)}\sum_{c\neq d}\lambda^2 = \lambda^2$$

and the first part of (7) holds. By (3), (iii), and the above equation

$$\mu_{a,b} = \frac{\ell_{a,b}}{\lambda} = \frac{\tilde{\ell}_{a,b}}{\lambda} = \frac{\tilde{\ell}_{a,b}}{\sqrt{\frac{1}{|A|(|A|-1)}\sum_{c\neq d}\frac{\overline{\mathrm{DT}}_{c,d}}{\varphi\left(\tilde{\ell}_{c,d}\right)}}}$$

for all $a \neq b$ in A.

(iv) implies (i). By the convention $\mu_{a,a} = \ell_{a,a} = 0$ for all $a \in A$, and the fact that $\mu_{a,b} = -\mu_{b,a}$ for all $a \neq b$ in a DDM, it follows that both ℓ and μ are antisymmetric. By Proposition 5, $\tilde{\ell}$ is cyclic. By the second part of (7), μ is cyclic too. Finally, Lemma 4 guarantees that the DDM is difference-based. ■

Proof of Corollary 2 Proposition 1 yields cyclicity of μ and Lemma 4 implies that (8) holds. ■

The triangle equality is easily seen to be equivalent to the product rule for the binary choice probabilities $P_{a,b}$ (for this rule, see Axiom EZ.2 in the Supplementary Appendix 5.2.2, and Baldassi et al. [24]). Therefore, a DDM is difference-based if and only if its binary choice probabilities satisfy the product rule. This rule is thus a further characterization, besides the triangle equality, of difference-based DDMs among general DDMs.

Proof of Proposition 3 Recall that data are generated by a difference-based DDM with parameters λ, $\mu_{a,b} = u\left(a\right) - u\left(b\right)$ for all $a, b \in A$, and $\sigma = \sqrt{2}$. We first show that the cyclic estimator is statistically consistent.

By the Strong Law of Large Numbers, the sample means of a (sequence of i.i.d. copies of a) random variable converge almost surely (a.s.) to its true mean. For each n, and all $a \neq b$ in A, $P^n_{a,b}$ is the n-th sample mean of a Bernoulli random variable with parameter

$$P_{a,b} = \frac{1}{1+e^{-\lambda(u(a)-u(b))}}$$

and $\overline{\mathrm{DT}}^n_{a,b}$ is the n-th sample mean of a random variable with mean

$$\overline{\mathrm{DT}}_{a,b} = \frac{\lambda}{u(a)-u(b)}\tanh\left(\lambda\frac{u(a)-u(b)}{2}\right)$$

Therefore, as $n \to \infty$,

$$P^n_{a,b} \xrightarrow{\text{a.s.}} P_{a,b} \quad \text{and} \quad \overline{\mathrm{DT}}^n_{a,b} \xrightarrow{\text{a.s.}} \overline{\mathrm{DT}}_{a,b} \tag{17}$$

Since the logarithm is a continuous function, by the continuous mapping theorem we have

$$\ell^n_{a,b} \xrightarrow{\text{a.s.}} \ell_{a,b} = \lambda(u(a)-u(b))$$

Thus,

$$\begin{aligned}\tilde{\ell}^n_{a,b} &= \frac{1}{|A|}\sum_{c\in A}\left(\ell^n_{a,c}+\ell^n_{c,b}\right) \xrightarrow{\text{a.s.}} \frac{1}{|A|}\sum_{c\in A}\left(\ell_{a,c}+\ell_{c,b}\right)\\ &= \frac{1}{|A|}\sum_{c\in A}\lambda(u(a)-u(c)+u(c)-u(b)) = \lambda(u(a)-u(b)) = \ell_{a,b}\end{aligned}$$

By continuity of φ, we also have

$$\tilde{\lambda}^n = \sqrt{\frac{1}{|A|(|A|-1)} \sum_{c \neq d} \frac{\overline{\mathrm{DT}}^n_{c,d}}{\varphi\left(\tilde{\ell}^n_{c,d}\right)}} \xrightarrow{\text{a.s.}} \sqrt{\frac{1}{|A|(|A|-1)} \sum_{c \neq d} \frac{\overline{\mathrm{DT}}_{c,d}}{\varphi\left(\ell_{c,d}\right)}}$$
$$= \sqrt{\frac{1}{|A|(|A|-1)} \sum_{c \neq d} \lambda^2} = \lambda$$

and

$$\tilde{\mu}^n_{a,b} = \frac{\tilde{\ell}^n_{a,b}}{\tilde{\lambda}^n} \xrightarrow{\text{a.s.}} \frac{\ell_{a,b}}{\lambda} = \mu_{a,b}$$

More formally, the limits of the sequences in (17) hold pointwise in sets of probability 1. Since there are $2|A|(|A|-1)$ such sets, the almost sure convergence of $\tilde{\ell}^n$, $\tilde{\lambda}^n$, and $\tilde{\mu}^n$ follows from the pointwise convergence of *all* the sequences in (17) on the intersection of the $2|A|(|A|-1)$ aforementioned sets, which is an event with probability 1.

Now that statistical consistence has been taken care of, we show that the cyclic estimator is value-consistent. In so doing, we restrict our attention to the case in which $P^n_{a,b} > 0$ for all $a \neq b$. In practice, when this is not the case $P^n_{a,b} = 0$ is replaced with a very small positive value ε and $P^n_{b,a}$ with $1 - \varepsilon$.

First observe that, by construction, $P^n_{a,b} = 1 - P^n_{b,a}$ for all $a \neq b$, but then

$$\ell^n_{a,b} = \ln \frac{P^n_{a,b}}{P^n_{b,a}} = -\ell^n_{b,a}$$

and ℓ^n is antysimmetric. Proposition 5 implies that

$$\tilde{\ell}^n_{a,b} = \frac{1}{|A|} \sum_{d \in A} \left(\ell^n_{a,d} + \ell^n_{d,b}\right)$$

is cyclic and so is $\tilde{\mu}^n = \tilde{\ell}^n / \tilde{\lambda}^n$.

This proves that the cyclic estimator is value-consistent. The final part of the statement follows immediately from Proposition 1. ■

The next example shows that when the triangle equality is violated, the utility functions defined in (8) by fixing different reference alternatives d rank alternatives in different, so inconsistent, ways.

Example 1. *Take a non-cyclic drift parameter μ, say with three alternatives, c, d, and d' such that*

$$\mu_{c,d} > 0 > \mu_{c,d'} + \mu_{d',d} \tag{18}$$

By taking d and d' as reference alternatives, we can define, as in (8), the utility functions

$$u(a) = \mu_{a,d} \qquad \forall a \in A$$
$$w(a) = \mu_{a,d'} \qquad \forall a \in A$$

Since $\mu_{c,d} > 0 = \mu_{dd}$, then

$$u(c) > u(d)$$

On the other hand, from $\mu_{c,d'} + \mu_{d',d} < 0$, it follows that $\mu_{c,d'} < -\mu_{d',d} = \mu_{d,d'}$, and so

$$w(c) < w(d)$$

Therefore the two utility functions rank the alternatives c and d differently.

The next example shows that empirical log-odds may be not cyclic, thus leading to the value-inconsistency of the plug-in estimator (9) described in Section 2.2.

Example 2. *Consider a difference-based DDM with $\lambda = 1$ and $u(c) = 1$, $u(d) = 3/4$, and $u(d') = 1/2$. The theoretical choice probabilities are*

$$P_{c,d} = P_{d,d'} \approx 0.56 \qquad \textit{and} \qquad P_{c,d'} \approx 0.62$$

Assume that the empirical probabilities realized by such a DDM over n trials satisfy

$$P^n_{c,d} > 1/2 \qquad \textit{and} \qquad P^n_{c,d'} < P^n_{d,d'}$$

This is not unlikely because of the relative small difference between the theoretical probabilities $P_{c,d'}$ and $P_{d,d'}$. We can now consider the plug-in estimator $\hat{\mu}^n : A \times A \to \mathbb{R}$ defined by

$$\hat{\mu}^n_{a,b} = \ell^n_{a,b} \qquad \forall\,(a,b) \in A \times A$$

Observe that

$$\hat{\mu}^n_{c,d} > 0 \qquad \textit{and} \qquad \hat{\mu}^n_{c,d'} < \hat{\mu}^n_{d,d'}$$

Therefore $\hat{\mu}^n_{c,d} > 0 > \hat{\mu}^n_{c,d'} + \hat{\mu}^n_{d',d}$ because $\hat{\mu}^n_{d',d} = -\hat{\mu}^n_{d,d'}$, and so the empirical log-odds are not cyclic. In particular, the triangle equality is violated as in (18) of Example 1. As a result, like in that example the estimated utility functions $\hat{u}(a) = \hat{\mu}^n_{a,d}$ and $\hat{w}(a) = \hat{\mu}^n_{a,d'}$ for all $a \in A$, are inconsistent (so fallacious) because

$$\hat{u}(c) > \hat{u}(d) \qquad \textit{and} \qquad \hat{w}(c) < \hat{w}(d)$$

5.2 Extensions of the cyclic estimator

5.2.1 Incomplete datasets

In this section we extend the cyclic estimator in order to deal with an incomplete dataset, as in Shevlin et al. [26]. We first discuss an example and then move to the general case. Throughout, we write $l_{x,y}$ instead of $\ell^n_{x,y}$ to ease notation, and when needed, we set $P^n_{x,x} = 1/2$, so that $l_{x,x} = 0$.

An example Assume that A consists of four alternatives a, b, c, d and that only the comparisons $\{a,b\}$, $\{b,c\}$, and $\{c,d\}$ are observed, say in the lab, as depicted in the graph below

$$\begin{array}{ccc} a & & d \\ \updownarrow & & \updownarrow \\ b & \leftrightarrow & c \end{array} \tag{19}$$

This is an instance when the observed choice behavior produces an empirical dataset of mean decision times $\overline{\mathrm{DT}}^n_{x,y}$, choice frequencies $P^n_{x,y}$, and log-odds $l_{x,y} = \log P^n_{x,y}/P^n_{y,x}$ for some but not all $x \neq y$ in A. For example, the comparison $\{a,c\}$ is missing in the dataset, hence $l_{a,c}$ is not defined. Thus, the adjusted log-odds formula (10), that is,

$$\widetilde{l}_{x,y} = \frac{1}{|A|} \sum_{z \in A} (l_{x,z} + l_{z,y})$$

cannot be computed. Yet, this formula can be extended to our incomplete dataset once we apply it to all pairs x, y for which there exists z in A such that both $l_{x,z}$ and $l_{z,y}$ are defined in the dataset. Formally, we have a generalized log-odds formula

$$\widetilde{l}_{x,y} = \frac{1}{|Z_{x,y}|} \sum_{z \in Z_{x,y}} (l_{x,z} + l_{z,y}) \tag{GLF}$$

where $Z_{x,y}$ is the set of all z such that $l_{x,z}$ and $l_{z,y}$ are defined in the dataset. In particular, the GLF is undefined when $Z_{x,y}$ is empty and, more interestingly, it reduces to (10) when the database is complete. So, it is a *bona fide* extension of the earlier formula.

We now apply the GLF to all pairs of alternatives appearing in graph (19). We will see that:

- for some connected pairs (like a, b) the GLF formula has no effect;
- for some disconnected pairs (like a, c) the GLF formula generates new adjusted log-odds and adds a link to the graph;
- for some disconnected pairs (like a, d) the GLF formula has no bite because the set $Z_{x,y}$ is empty.

Let us start with the pair a, b. The only elements z for which both $l_{a,z}$ and $l_{z,b}$ are defined are $z = a$ and $z = b$ themselves. By the GLF,

$$\widetilde{l}_{a,b} = \frac{1}{2}(l_{a,a} + l_{a,b}) + \frac{1}{2}(l_{a,b} + l_{b,b}) = l_{a,b}$$

By coloring in purple the links which we have applied the GLF to, we obtain

$$\begin{array}{ccc} a & & d \\ \textcolor{purple}{\updownarrow} & & \updownarrow \\ b & \leftrightarrow & c \end{array}$$

Moving to the pair a, c, the element $z = b$ is the only one for which both $l_{a,z}$ and $l_{z,c}$ are defined in the dataset of the original graph (19). In this case, by applying the GLF we define the adjusted log-odds

$$\widetilde{l}_{a,c} = l_{a,b} + l_{b,c}$$

This amounts to adding a new link $a \leftrightarrow c$ to the graph

$$\begin{array}{ccc} a & & d \\ \updownarrow & \searrow & \updownarrow \\ b & \leftrightarrow & c \end{array}$$

This addition of a link is impossible for the pair a, d because there is no z in the original graph (19) for which both $l_{a,z}$ and $l_{z,d}$ are defined – i.e., the set $Z_{a,d}$ is empty.

The situation for the pairs b, c and c, d, in the original graph (19) is similar to that of a, b. Instead, the pair b, d can now be connected as we did for a, c. Specifically,

$$\widetilde{l}_{b,c} = \frac{1}{2}(l_{b,b} + l_{b,c}) + \frac{1}{2}(l_{b,c} + l_{c,c}) = l_{b,c}$$
$$\widetilde{l}_{c,d} = \frac{1}{2}(l_{c,c} + l_{c,d}) + \frac{1}{2}(l_{c,d} + l_{d,d}) = l_{c,d}$$
$$\widetilde{l}_{b,d} = l_{b,c} + l_{c,d}$$

This leads to a new augmented graph

$$\begin{array}{ccc} a & & d \\ \updownarrow & \diagup\!\!\diagdown & \updownarrow \\ b & \leftrightarrow & c \end{array} \tag{20}$$

with (adjusted) choice frequencies

$$\widetilde{P}_{x,y} = \frac{1}{1 + e^{-\widetilde{l}_{x,y}}}$$

for all the connected pairs of alternatives.

Graph (20) is still incomplete since the comparison $\{a, d\}$ is missing. But, a second application of the GLF, this time to $\widetilde{l}$ rather than to l, leads to a complete graph and, correspondingly, to a dataset in which all log-odds $\widetilde{\widetilde{l}}_{x,y}$ are defined. Specifically, in graph (20) there are two elements z such that $\widetilde{l}_{a,z}$ and $\widetilde{l}_{z,d}$ are defined: $z = b$ and $z = c$. By the GLF,

$$\widetilde{\widetilde{l}}_{a,d} = \frac{1}{2}(\widetilde{l}_{a,b} + \widetilde{l}_{b,d}) + \frac{1}{2}(\widetilde{l}_{a,c} + \widetilde{l}_{c,d})$$

These adjusted log-odds provide the missing link $a \leftrightarrow d$. Graphically,

$$\begin{array}{ccc} a & \leftrightarrow & d \\ \updownarrow & \diagup\!\!\diagdown & \updownarrow \\ b & \leftrightarrow & c \end{array}$$

Now the GLF must be applied for a second time to all remaining pairs in (20). For example,

$$\widetilde{\widetilde{l}}_{b,c} = \frac{1}{4}(\widetilde{l}_{b,a} + \widetilde{l}_{a,c}) + \frac{1}{4}(\widetilde{l}_{b,b} + \widetilde{l}_{b,c}) + \frac{1}{4}(\widetilde{l}_{b,c} + \widetilde{l}_{c,c}) + \frac{1}{4}(\widetilde{l}_{b,d} + \widetilde{l}_{d,c})$$

By proceeding in this way, the new augmented graph

$$\begin{array}{ccc} a & \leftrightarrow & d \\ \updownarrow & \diagup\!\!\diagdown & \updownarrow \\ b & \leftrightarrow & c \end{array} \tag{21}$$

is obtained, with

$$\widetilde{\widetilde{P}}_{x,y} = \frac{1}{1 + e^{-\widetilde{\widetilde{l}}_{x,y}}}$$

Graph (21) is complete, with $\widetilde{\widetilde{l}}_{x,y}$ defined for all x, y in A. Yet, $\widetilde{\widetilde{l}}$ may not satisfy the triangle equality. A third application of the GLF, now equivalent to formula (10) thanks to completeness, leads to adjusted log-odds

$$\widetilde{\widetilde{\widetilde{l}}}_{x,y} = \frac{1}{|4|} \sum_{z \in \{a,b,c,d\}} \left(\widetilde{\widetilde{l}}_{x,z} + \widetilde{\widetilde{l}}_{z,y} \right)$$

for all x, y in A. As these log-odds satisfy the triangle equality, the completion procedure is finished.

The general case Given the set A of alternatives, an *experiment* is a collection of choice episodes

$$\{(\{x_i, y_i\}, z_i, t_i) : i = 1, ..., m\}$$

where $\{x_i, y_i\}$ is the unordered pair of distinct alternatives in A compared in episode i of the experiment, $z_i \in \{x_i, y_i\}$ is the observed outcome of the comparison, and t_i is the observed DT. The graph $\mathcal{G}$ defined by this experiment is the collection of all pairs $\{a, b\}$ that are directly compared

$$a \leftrightarrow b$$

in some episode. This graph is the general counterpart of the graph (19) of the previous example.

For each $\{a, b\}$ in $\mathcal{G}$, the set of episodes featuring comparison $a \leftrightarrow b$ is

$$I_{a,b} = \{i \in \{1, ..., m\} : \{x_i, y_i\} = \{a, b\}\}$$

We have

$$P_{a,b}^{|I_{a,b}|} = \frac{1}{|I_{a,b}|} \sum_{i \in I_{a,b}} \delta_{z_i a} \quad ; \quad P_{b,a}^{|I_{a,b}|} = \frac{1}{|I_{a,b}|} \sum_{i \in I_{a,b}} \delta_{z_i b} \quad ; \quad \overline{\mathrm{DT}}_{a,b}^{|I_{a,b}|} = \frac{1}{|I_{a,b}|} \sum_{i \in I_{a,b}} t_i$$

where δ_{xy} is the *Kronecker delta* taking value 1 if $x = y$ and value 0 otherwise.

We can extend formula (10) by maintaining the simplified notation $l_{x,y}$ for $\ell_{x,y}^{|I_{a,b}|}$ and by setting

$$\tilde{l}_{a,b} = \frac{1}{|Z_{a,b}|} \sum_{z \in Z_{a,b}} (l_{a,z} + l_{z,b}) \tag{GLF}$$

for all a, b in A such that the set $Z_{a,b}$ of all z for which $l_{a,z}$ and $l_{z,b}$ are defined in the dataset is not empty. By iterating k-times the GLF, we impute values $\tilde{l}^{k}_{a,b}$ to all pairs a, b in A for which there is at least a chain of comparisons

$$a = c_0 \leftrightarrow c_1 \leftrightarrow ... \leftrightarrow c_{k+1} = b$$

Therefore, if the original graph $\mathcal{G}$ is connected, in at most $|A|$ iterations we obtain an imputation $\tilde{l}^{|A|}_{a,b}$ of adjusted log-odds that satisfy the triangle equality (when $\mathcal{G}$ is not connected, the same analysis applies to all of its connected components).

Having extended formula (10), we can extend the definition of cyclic estimator to incomplete datasets.

Definition 4. *The* cyclic estimator *of a difference based DDM is given by*

$$\tilde{\lambda} = \sqrt{\frac{1}{|\mathcal{G}|} \sum_{\{c,d\} \in \mathcal{G}} \frac{\overline{\mathrm{DT}}_{c,d}^{|I_{c,d}|}}{\varphi\left(\tilde{l}^{|A|}_{c,d}\right)}} \qquad \textit{and} \qquad \tilde{\mu}_{a,b} = \frac{\tilde{l}^{|A|}_{a,b}}{\tilde{\lambda}} \tag{22}$$

for all alternatives a and b in A.

5.2.2 Nondecision times

In behavioral experiments the analyst typically does not observe a DT but, rather, a RT which is the sum of the DT and of the time needed to encode the stimuli and execute the response, called *latency* or *nondecision time*.

An augmented DDM, called EZ-DDM by Wagenmakers et al. [63], permits to tackle this difficulty. For all $a \neq b$ in A, it considers the random variables $Z_{a,b}(t)$, $\mathrm{DT}_{a,b}$, and $\mathrm{DO}_{a,b}$ introduced in the main text, as well as a latency $T_{a,b} \geq 0$ that permits to define a *reaction time*

$$\mathrm{RT}_{a,b} = T_{a,b} + \mathrm{DT}_{a,b}$$

We denote by $\mathrm{EZ}(u, \lambda, T)$ an EZ-DDM with parameters $u : A \to \mathbb{R}$, $\lambda > 0$, and $T : A^2_{\neq} \to [0, \infty)$, where $T_{a,b} = T_{b,a}$ is the nondecision time of comparison $\{a, b\}$. Specifically, the set $A^2_{\neq}$ is the collection of all ordered pairs of distinct alternatives in A; moreover, it is convenient to directly use a utility u rather than a cyclic drift parameter μ, having established the equivalence of the two approaches. To extend the cyclic estimator to the EZ-DDM, we first need to extend the DDM axiomatic analysis of Baldassi et al. [24] by finding necessary and sufficient conditions on "asymptotic observables" which characterize a $\mathrm{EZ}(u, \lambda, T)$ generating them. For all $a \neq b$ in A, these observables are:

- $P^{\infty}_{a,b}$ the (limit) frequency with which a is chosen over b;
- $\mathrm{MRT}^{\infty}_{a,b}$ the (limit) average RT in the comparison of a and b;
- $\mathrm{VRT}^{\infty}_{a,b}$ the (limit) variance of RT in the comparison of a and b.

More formally, we call *asymptotic observables* any triplet $(P^{\infty}, \mathrm{MRT}^{\infty}, \mathrm{VRT}^{\infty})$ of square matrices

$$\left\{ \left[P^{\infty}_{a,b}, \mathrm{MRT}^{\infty}_{a,b}, \mathrm{VRT}^{\infty}_{a,b} \right]_{a \neq b} : \forall a \neq b, P^{\infty}_{a,b} + P^{\infty}_{b,a} = 1, \mathrm{MRT}^{\infty}_{a,b} = \mathrm{MRT}^{\infty}_{b,a}, \mathrm{VRT}^{\infty}_{a,b} = \mathrm{VRT}^{\infty}_{b,a} \right\}$$

Again, we set $P^{\infty}_{a,a} = 1/2$ and leave undefined $\mathrm{MRT}^{\infty}_{a,a}$ and $\mathrm{VRT}^{\infty}_{a,a}$. The idea of using these limit quantities to analyze forced choice tasks dates back to Cattell [64].

To ease notation, we denote the (limit) log-odds for a against b by $\ell^{\infty}_{a,b} = \log P^{\infty}_{a,b}/P^{\infty}_{b,a}$. The following axioms, in the spirit of Baldassi et al. [24] and informed by Wagenmakers et al. [63], are required to hold for all distinct $a, b, c \in A$.

EZ. 1 (Positivity)**.** $P^{\infty}_{a,b} > 0$*,* $\mathrm{MRT}^{\infty}_{a,b} > 0$*, and* $\mathrm{VRT}^{\infty}_{a,b} > 0$*.*

EZ. 2 (Product rule)**.** $P^{\infty}_{c,a} P^{\infty}_{b,c} P^{\infty}_{a,b} = P^{\infty}_{b,a} P^{\infty}_{c,b} P^{\infty}_{a,c}$*.*

EZ. 3 (Invariance)**.** $\mathrm{VRT}^{\infty}_{a,b} \dfrac{\left(e^{\ell^{\infty}_{a,b}} + 1\right)^2 \left(\ell^{\infty}_{a,b}\right)^3}{e^{2\ell^{\infty}_{a,b}} - 2\ell^{\infty}_{a,b} e^{\ell^{\infty}_{a,b}} - 1} = \mathrm{VRT}^{\infty}_{a,c} \dfrac{\left(e^{\ell^{\infty}_{a,c}} + 1\right)^2 \left(\ell^{\infty}_{a,c}\right)^3}{e^{2\ell^{\infty}_{a,c}} - 2\ell^{\infty}_{a,c} e^{\ell^{\infty}_{a,c}} - 1}$.

EZ. 4 (Solvability)**.** $2\left(\mathrm{MRT}^{\infty}_{a,b}\right)^2 \geq \mathrm{VRT}^{\infty}_{a,b} \dfrac{\left(e^{\ell^{\infty}_{a,b}} - 1\right)^2 \ell^{\infty}_{a,b}}{e^{2\ell^{\infty}_{a,b}} - 2\ell^{\infty}_{a,b} e^{\ell^{\infty}_{a,b}} - 1}$.

Axioms EZ.1 and EZ.2 are classical psychometric axioms, while axioms EZ.3 and EZ.4 are technical and inspired by the non-axiomatic analysis of Wagenmakers et al. [63].

Theorem 6. *The following statements are equivalent:*

(i) the asymptotic observables $(P^{\infty}, \mathrm{MRT}^{\infty}, \mathrm{VRT}^{\infty})$ *satisfy EZ.1, EZ.2, EZ.3, and EZ.4;*

(ii) there exist a function $u : A \to \mathbb{R}$*, a threshold* $\lambda > 0$*, and a symmetric function* $T : A^2_{\neq} \to [0, \infty)$ *such that* P^{∞}*,* MRT^{∞}*, and* VRT^{∞} *are the choice probabilities, mean RT, and RT variances of* $\mathrm{EZ}(u, \lambda, T)$*.*

In this case, λ *is unique, and* u *is unique up to an additive constant. In particular,*

$$\lambda = \sqrt[4]{\frac{\mathrm{VRT}^{\infty}_{a,b}}{2} \frac{\left(e^{\ell^{\infty}_{a,b}} + 1\right)^2 \left(\ell^{\infty}_{a,b}\right)^3}{e^{2\ell^{\infty}_{a,b}} - 2\ell^{\infty}_{a,b} e^{\ell^{\infty}_{a,b}} - 1}} \qquad \text{and} \qquad u(a) - u(b) = \frac{\ell^{\infty}_{a,b}}{\lambda}$$

for all $a \neq b$ *in* A*. Moreover,* T *is unique and given by*

$$T_{a,b} = \mathrm{MRT}^{\infty}_{a,b} - \sqrt{\frac{\mathrm{VRT}^{\infty}_{a,b}}{2} \frac{\left(e^{\ell^{\infty}_{a,b}} - 1\right)^2 \ell^{\infty}_{a,b}}{e^{2\ell^{\infty}_{a,b}} - 2\ell^{\infty}_{a,b} e^{\ell^{\infty}_{a,b}} - 1}}$$

for all $a \neq b$ *in* A*.*

Clearly, the DDM is the special case when $T_{a,b} = 0$ for all $a \neq b$. Thus, this theorem provides a characterization of the DDM based on reaction times' means and variances which is alternative to that of Baldassi et al. [24]. The axiom delivering the DDM is obtained by replacing the inequality in EZ.4 with an equality.

Proof (i) implies (ii). By EZ.1, we have that $\ell^{\infty}_{a,b} \in \mathbb{R}$, for all $a \neq b$ in A. Arbitrarily choose $c \in A$, set $v(c) = 0$ and

$$v(a) = \ell^{\infty}_{a,c} \tag{23}$$

for all $a \neq c$ in A. Then, for all $a \neq b$ in $A \setminus \{c\}$, by EZ.2, we have

$$\ell^{\infty}_{a,b} = \ell^{\infty}_{a,c} - \ell^{\infty}_{b,c} = v(a) - v(b)$$

and direct application of (23) delivers the same result for $a = c \neq b$ and for $b = c \neq a$. Then $P^{\infty}_{a,b} = 1/\left(1 + e^{-\ell^{\infty}_{a,b}}\right)$ implies

$$P^{\infty}_{a,b} = \frac{1}{1 + e^{-[v(a) - v(b)]}}$$

for all $a \neq b$ in A.

Tedious verification shows that axiom EZ.3 guarantees that

$$\mathrm{VRT}^{\infty}_{a,b} \frac{\left(e^{\ell^{\infty}_{a,b}} + 1\right)^2 \left(\ell^{\infty}_{a,b}\right)^3}{e^{2\ell^{\infty}_{a,b}} - 2\ell^{\infty}_{a,b} e^{\ell^{\infty}_{a,b}} - 1} = \mathrm{VRT}^{\infty}_{a',b'} \frac{\left(e^{\ell^{\infty}_{a',b'}} + 1\right)^2 \left(\ell^{\infty}_{a',b'}\right)^3}{e^{2\ell^{\infty}_{a',b'}} - 2\ell^{\infty}_{a',b'} e^{\ell^{\infty}_{a',b'}} - 1} \tag{24}$$

for all $a \neq b$ and all $a' \neq b'$ in A; and not only if $a' = a$ as the axiom requires.

Specifically, define

$$f(a,b) = \mathrm{VRT}^{\infty}_{a,b} \frac{\left(e^{\ell^{\infty}_{a,b}} + 1\right)^2 \left(\ell^{\infty}_{a,b}\right)^3}{e^{2\ell^{\infty}_{a,b}} - 2\ell^{\infty}_{a,b} e^{\ell^{\infty}_{a,b}} - 1} \qquad \forall (a,b) \in A^2_{\neq}$$

By EZ.3,

$$f(a,b) = f(a,c) \qquad \forall (a,b), (a,c) \in A^2_{\neq} : b \neq c \tag{25}$$

Of course, the same holds when $b = c$. Moreover, for all $(a,b) \in A^2_{\neq}$,

$$f(a,b) = \mathrm{VRT}^{\infty}_{a,b} \frac{\left(e^{\ell^{\infty}_{a,b}} + 1\right)^2 \left(\ell^{\infty}_{a,b}\right)^3}{e^{2\ell^{\infty}_{a,b}} - 2\ell^{\infty}_{a,b} e^{\ell^{\infty}_{a,b}} - 1} = \mathrm{VRT}^{\infty}_{b,a} \frac{\left(e^{-\ell^{\infty}_{b,a}} + 1\right)^2 \left(-\ell^{\infty}_{b,a}\right)^3}{e^{-2\ell^{\infty}_{b,a}} - 2\left(-\ell^{\infty}_{b,a}\right) e^{-\ell^{\infty}_{b,a}} - 1}$$

but

$$\frac{-\left(e^{-x} + 1\right)^2 x^3}{e^{-2x} + 2xe^{-x} - 1} = \frac{\left(e^{x} + 1\right)^2 x^3}{e^{2x} - 2xe^{x} - 1} \qquad \forall x \in \mathbb{R} \tag{26}$$

Thus,

$$\mathrm{VRT}^{\infty}_{b,a} \frac{\left(e^{-\ell^{\infty}_{b,a}} + 1\right)^2 \left(-\ell^{\infty}_{b,a}\right)^3}{e^{-2\ell^{\infty}_{b,a}} - 2\left(-\ell^{\infty}_{b,a}\right) e^{-\ell^{\infty}_{b,a}} - 1} = \mathrm{VRT}^{\infty}_{b,a} \frac{\left(e^{\ell^{\infty}_{b,a}} + 1\right)^2 \left(\ell^{\infty}_{b,a}\right)^3}{e^{2\ell^{\infty}_{b,a}} - 2\ell^{\infty}_{b,a} e^{\ell^{\infty}_{b,a}} - 1} = f(b,a)$$

that is,

$$f(a,b) = f(b,a) \tag{27}$$

Now, since f satisfies (25) and (27), then f is constant.

In fact, for all $(a,b), (c,d) \in A^2_{\neq}$,

$$f(a,b) = f(a,c) = f(c,a) = f(c,d)$$

where the first equality follows from (25), the second from (27), and the third from (25) again.

Now, arbitrarily choose $a' \neq b'$ in A and define

$$2\lambda^4 = \mathrm{VRT}^{\infty}_{a',b'} \frac{\left(e^{\ell^{\infty}_{a',b'}} + 1\right)^2 \left(\ell^{\infty}_{a',b'}\right)^3}{e^{2\ell^{\infty}_{a',b'}} - 2\ell^{\infty}_{a',b'} e^{\ell^{\infty}_{a',b'}} - 1} \tag{28}$$

and $u(a) = v(a)/\lambda$ for all a in A, so that $v = \lambda u$. It follows that, for all $a \neq b$ in A,

$$P^{\infty}_{a,b} = \frac{1}{1 + e^{-[v(a) - v(b)]}} = \frac{1}{1 + e^{-\lambda[u(a) - u(b)]}} = P_{a,b}$$

where $P_{a,b}$ is the choice frequency induced by $\mathrm{EZ}(u, \lambda, T)$, irrespective of T. Then, recalling $\ell^{\infty}_{a,b} = \lambda[u(a) - u(b)] = \lambda\Delta$ and using (24) and (28), it follows that, for all $a \neq b$ in A,

$$\mathrm{VRT}^{\infty}_{a,b} = 2\lambda^4 \frac{e^{2\ell^{\infty}_{a,b}} - 2\ell^{\infty}_{a,b} e^{\ell^{\infty}_{a,b}} - 1}{\left(e^{\ell^{\infty}_{a,b}} + 1\right)^2 \left(\ell^{\infty}_{a,b}\right)^3} = 2\lambda^4 \frac{e^{2\lambda\Delta} - 2\lambda\Delta e^{\lambda\Delta} - 1}{\left(e^{\lambda\Delta} + 1\right)^2 (\lambda\Delta)^3} \tag{29}$$

But Wagenmakers et al. [63] prove that, when $\mathrm{EZ}(u,\lambda\,,T)$ is considered,

$$\mathrm{VRT}_{a,b} = \frac{2\lambda\sigma^2}{2\Delta^3}\frac{2\xi e^{\xi} - e^{2\xi} + 1}{\left(e^{\xi}+1\right)^2}$$

where $\xi = -2\lambda\Delta/\sigma^2$ and, in our case, $\sigma^2 = 2$, so that $\xi = -\lambda\Delta$ and

$$\begin{aligned}\mathrm{VRT}_{a,b} &= \frac{4\lambda}{2\Delta^3}\frac{-2\lambda\Delta e^{-\lambda\Delta} - e^{-2\lambda\Delta} + 1}{\left(e^{-\lambda\Delta}+1\right)^2} = 2\lambda^4\frac{-2\lambda\Delta e^{-\lambda\Delta} - e^{-2\lambda\Delta} + 1}{\left(e^{-\lambda\Delta}+1\right)^2(\lambda\Delta)^3}\\ &= 2\lambda^4\frac{e^{-2\lambda\Delta} + 2\lambda\Delta e^{-\lambda\Delta} - 1}{-\left(e^{-\lambda\Delta}+1\right)^2(\lambda\Delta)^3}\end{aligned}$$

and (26) yields $\mathrm{VRT}^{\infty}_{a,b} = \mathrm{VRT}_{a,b}$.

Moreover, defining

$$T_{a,b} = \mathrm{MRT}^{\infty}_{a,b} - \sqrt{\frac{\mathrm{VRT}^{\infty}_{a,b}}{2}\frac{\left(e^{\ell^{\infty}_{a,b}}-1\right)^2\ell^{\infty}_{a,b}}{e^{2\ell^{\infty}_{a,b}} - 2\ell^{\infty}_{a,b}e^{\ell^{\infty}_{a,b}} - 1}}$$

for all $a \neq b$ in A, it follows that $T_{a,b}$ is positive thanks to EZ.4, and

$$\mathrm{MRT}^{\infty}_{a,b} = T_{a,b} + \sqrt{\frac{\mathrm{VRT}^{\infty}_{a,b}}{2}\frac{\left(e^{\ell^{\infty}_{a,b}}-1\right)^2\ell^{\infty}_{a,b}}{e^{2\ell^{\infty}_{a,b}} - 2\ell^{\infty}_{a,b}e^{\ell^{\infty}_{a,b}} - 1}} = T_{a,b} + \sqrt{\frac{\mathrm{VRT}^{\infty}_{a,b}}{2}\frac{\left(e^{\lambda\Delta}-1\right)^2\lambda\Delta}{e^{2\lambda\Delta} - 2\lambda\Delta e^{\lambda\Delta} - 1}}$$

Using (29), this implies

$$\begin{aligned}\mathrm{MRT}^{\infty}_{a,b} &= T_{a,b} + \sqrt{\lambda^4\frac{e^{2\lambda\Delta} - 2\lambda\Delta e^{\lambda\Delta} - 1}{\left(e^{\lambda\Delta}+1\right)^2(\lambda\Delta)^3}\frac{\left(e^{\lambda\Delta}-1\right)^2\lambda\Delta}{e^{2\lambda\Delta} - 2\lambda\Delta e^{\lambda\Delta} - 1}}\\ &= T_{a,b} + \sqrt{\frac{\lambda^4}{\lambda^2\Delta^2}\frac{\left(e^{\lambda\Delta}-1\right)^2}{\left(e^{\lambda\Delta}+1\right)^2}} = T_{a,b} + \lambda^2\sqrt{\frac{1}{\lambda^2\Delta^2}\frac{\left(e^{\lambda\Delta}-1\right)^2}{\left(e^{\lambda\Delta}+1\right)^2}}\\ &= T_{a,b} + \lambda^2\left|\frac{1}{\lambda\Delta}\frac{e^{\lambda\Delta}-1}{e^{\lambda\Delta}+1}\right| = T_{a,b} + \frac{\lambda}{\Delta}\frac{e^{\lambda\Delta}-1}{e^{\lambda\Delta}+1}\end{aligned}$$

But, when $\mathrm{EZ}(u,\lambda\,,T)$ is considered,

$$\mathrm{MRT}_{a,b} = T_{a,b} + \overline{\mathrm{DT}}_{a,b} = T_{a,b} + \frac{\lambda}{\Delta}\tanh\left(\frac{\lambda\Delta}{2}\right) = T_{a,b} + \frac{\lambda}{\Delta}\frac{e^{\lambda\Delta}-1}{e^{\lambda\Delta}+1}$$

showing that $\mathrm{MRT}^{\infty}_{a,b} = \mathrm{MRT}_{a,b}$. Thus (ii) holds for the EZ-DDM with parameters u, λ, and T.

(ii) implies (i), and uniqueness. Assume that there exist a function $u : A \to \mathbb{R}$, a threshold $\lambda > 0$, and a symmetric function $T : A^2_{\neq} \to [0,\infty)$ such that P^{∞}, MRT^{∞}, and VRT^{∞} are the choice probabilities, mean RT, and RT variances of $\mathrm{EZ}\,(u,\lambda\,,T)$. This means that, for all $a \neq b$ in A,

$$\begin{aligned}P^{\infty}_{a,b} &= P_{a,b} = \frac{1}{1+e^{-\lambda[u(a)-u(b)]}}\ \text{(and so } \lambda\Delta = \ell^{\infty}_{a,b})\\ \mathrm{MRT}^{\infty}_{a,b} &= \mathrm{MRT}_{a,b} = T_{a,b} + \overline{\mathrm{DT}}_{a,b} = T_{a,b} + \frac{\lambda^2}{\lambda\Delta}\frac{e^{\lambda\Delta}-1}{e^{\lambda\Delta}+1}\\ \mathrm{VRT}^{\infty}_{a,b} &= \mathrm{VRT}_{a,b} = 2\lambda^4\frac{e^{2\lambda\Delta} - 2\lambda\Delta e^{\lambda\Delta} - 1}{\left(e^{\lambda\Delta}+1\right)^2(\lambda\Delta)^3}\end{aligned}$$

Then $P^{\infty}_{a,b} > 0$, and since

$$\frac{1}{x}\frac{e^x-1}{e^x+1} > 0 \qquad \text{and} \qquad \frac{e^{2x} - 2xe^x - 1}{\left(e^x+1\right)^2x^3} > 0 \qquad \forall x \in \mathbb{R}$$

we also have $\mathrm{MRT}^{\infty}_{a,b} > 0$ and $\mathrm{VRT}^{\infty}_{a,b} > 0$, so that EZ.1 is satisfied.

Since

$$P^{\infty}_{a,b} = \frac{e^{\lambda u(a)}}{e^{\lambda u(a)} + e^{\lambda u(b)}}$$

the verification of EZ.2 is routine.

Moreover, given any $a \neq b$ and $c \neq d$, and recalling $\lambda\left[u\left(x\right) - u\left(y\right)\right] = \ell^{\infty}_{x,y}$, we have

$$\frac{\mathrm{VRT}^{\infty}_{a,b}}{2}\frac{\left(e^{\ell^{\infty}_{a,b}}+1\right)^2\left(\ell^{\infty}_{a,b}\right)^3}{e^{2\ell^{\infty}_{a,b}} - 2\ell^{\infty}_{a,b}e^{\ell^{\infty}_{a,b}} - 1} = \lambda^4 = \frac{\mathrm{VRT}^{\infty}_{c,d}}{2}\frac{\left(e^{\ell^{\infty}_{c,d}}+1\right)^2\left(\ell^{\infty}_{c,d}\right)^3}{e^{2\ell^{\infty}_{c,d}} - 2\ell^{\infty}_{c,d}e^{\ell^{\infty}_{c,d}} - 1}$$

this yields, simultaneously, uniqueness of λ and verification of EZ.3. But then

$$u\left(x\right) - u\left(y\right) = \frac{\ell^{\infty}_{x,y}}{\lambda}$$

yields uniqueness of u up to an additive constant.

Finally,

$$\begin{aligned}
\mathrm{MRT}^{\infty}_{a,b} &= \mathrm{MRT}_{a,b} = T_{a,b} + \frac{\lambda^2}{\lambda\Delta}\frac{e^{\lambda\Delta}-1}{e^{\lambda\Delta}+1} = T_{a,b} + \sqrt{\lambda^4\frac{e^{2\lambda\Delta} - 2\lambda\Delta e^{\lambda\Delta} - 1}{\left(e^{\lambda\Delta}+1\right)^2\left(\lambda\Delta\right)^3}\frac{\left(e^{\lambda\Delta}-1\right)^2\lambda\Delta}{e^{2\lambda\Delta} - 2\lambda\Delta e^{\lambda\Delta} - 1}} \\
&= T_{a,b} + \sqrt{\lambda^4\frac{e^{2\ell^{\infty}_{a,b}} - 2\ell^{\infty}_{a,b}e^{\ell^{\infty}_{a,b}} - 1}{\left(e^{\ell^{\infty}_{a,b}}+1\right)^2\left(\ell^{\infty}_{a,b}\right)^3}\frac{\left(e^{\ell^{\infty}_{a,b}}-1\right)^2\ell^{\infty}_{a,b}}{e^{2\ell^{\infty}_{a,b}} - 2\ell^{\infty}_{a,b}e^{\ell^{\infty}_{a,b}} - 1}} = T_{a,b} + \sqrt{\frac{\mathrm{VRT}^{\infty}_{a,b}}{2}\frac{\left(e^{\ell^{\infty}_{a,b}}-1\right)^2\ell^{\infty}_{a,b}}{e^{2\ell^{\infty}_{a,b}} - 2\ell^{\infty}_{a,b}e^{\ell^{\infty}_{a,b}} - 1}}
\end{aligned}$$

implies that T is unique and that

$$\mathrm{MRT}^{\infty}_{a,b} \geq \sqrt{\frac{\mathrm{VRT}^{\infty}_{a,b}}{2}\frac{\left(e^{\ell^{\infty}_{a,b}}-1\right)^2\ell^{\infty}_{a,b}}{e^{2\ell^{\infty}_{a,b}} - 2\ell^{\infty}_{a,b}e^{\ell^{\infty}_{a,b}} - 1}}$$

hence EZ.4 follows. ■

This theorem is the EZ-DDM counterpart of the DDM Theorem of Baldassi et. [24]. It allows us to generalize the definition of the cyclic estimator to account for latency. Indeed, if we assume that the analyst observes the empirical choice frequencies $P^{n}_{a,b}$, empirical mean reaction times $\mathrm{MRT}^{n}_{a,b}$, and empirical variances $\mathrm{VRT}^{n}_{a,b}$, then we can define $\tilde{\ell}^{n}_{a,b}$ by formula (10) and obtain an augmented estimator.

Definition 5. *The* augmented cyclic estimator *of an EZ-DDM is given by*

$$\tilde{\lambda} = \sqrt[4]{\frac{1}{|A|(|A|-1)}\sum_{c\neq d}\frac{\mathrm{VRT}^{n}_{c,d}}{2}\frac{\left(e^{\tilde{\ell}^{n}_{c,d}}+1\right)^2\left(\tilde{\ell}^{n}_{c,d}\right)^3}{e^{2\tilde{\ell}^{n}_{c,d}} - 2\tilde{\ell}^{n}_{c,d}e^{\tilde{\ell}^{n}_{c,d}} - 1}}$$

$$\tilde{u}\left(a\right) - \tilde{u}\left(b\right) = \frac{\tilde{\ell}^{n}_{c,d}}{\tilde{\lambda}}$$

$$\tilde{T}_{a,b} = \mathrm{MRT}^{n}_{a,b} - \sqrt{\frac{\mathrm{VRT}^{n}_{a,b}}{2}\frac{\left(e^{\tilde{\ell}^{n}_{a,b}}-1\right)^2\tilde{\ell}^{n}_{a,b}}{e^{2\tilde{\ell}^{n}_{a,b}} - 2\tilde{\ell}^{n}_{a,b}e^{\tilde{\ell}^{n}_{a,b}} - 1}}$$

for all distinct alternatives a and b in A.

The consistency properties of this estimator and the possibility of extending it to incomplete datasets are totally analogous to the ones of the cyclic estimator.

5.2.3 Biased DDMs

The DDMs that we considered in the previous sections have been assumed to be *unbiased*, with no prior inclination towards one of the two alternatives. Mathematically, this means that the net evidence process (1) is assumed to start at 0. The case of biased DDMs is a bit more involved, due to the fact that no closed form expression for their parameters as functions of choice frequencies and RT moments is available. Nonetheless, we conjecture that a combination of our ideas and those of Wagenmakers et al. [63] might lead to an extension of the cyclic estimator to this case too. This approach is left for future research.

5.3 Model comparison

In the main text we presented the results of our cyclic estimator, as well as comparisons to two other methods.

The first alternative method that we considered was logistic regression. We regressed a binary choice variable (1 = correct, 0 = incorrect) on dummy variables for each possible value (1 = value for correct option, -1 = value for incorrect option, 0 = value not present). Like with the cyclic estimator, we assumed that all the data came from a single subject; we did not include random effects or other cluster corrections.

The second alternative method that we considered was HDDM (version 0.8.0), a hierarchical Bayesian toolbox for fitting the DDM to data [34]. The boundaries of the DDM were set to be upper = correct and lower = incorrect. Drift rate was specified as a regression analogous to the logistic regression above, with dummy variables for each possible value (1 = value for correct option, -1 = value for incorrect option, 0 = value not present). We set the drift-rate intercept, starting-point bias, all across-trial variability parameters, and the outlier probability to zero. In summary, we estimated boundary separation, non-decision time, and utilities for each option in the drift rate function. We used 4 chains, each with 6000 samples after 4000 samples of warm-up. Priors were set to their default values. All R-hat values were less than 1.01, indicating convergence.

In the following sections we compare these two alternative methods to our cyclic estimator for the subject-level data, and simulated data.

5.3.1 Individual choice data

In the main text we presented the results of DDMs fit to data pooled across subjects. However, the DDM is often fit to individual subjects. Here we present the results of DDMs fit to subject-level data in the Cavanagh et al. [25] and Shevlin et al. [26] datasets. For the Cavanagh et al. [25] data we present the utility estimates for all 20 subjects (Fig. S1). For the Shevlin et al. [26] data there are too many plots to include them all - there are 70 subjects with 3 value tiers each, i.e., 210 plots total. Instead, we present 12 randomly selected plots, 4 from each value tier (Fig. S2).

We can also compare the estimators quantitatively. To do so, we calculated their average absolute deviation from the diagonal line (i.e., linear utility) for each subject, and then tested whether they were significantly different from each other using a non-parametric paired Mann-Whitney-Wilcoxon test (since these measures were not normally distributed).

In the Cavanagh et al. [25] data there was no significant difference between the cyclic and logistic estimators ($p = 0.18$). This indicates that our estimator did no worse, but no better than, a standard logistic regression. The HDDM estimator outperformed both the logistic estimator ($p = 0.02$) and the cyclic estimator ($p = 0.003$), presumably because it included more data in the estimates; HDDM fits the DDM hierarchically using all the subjects' data and it also uses RT to infer drift rates. The Cavanagh et al. [25] dataset is also a case where every pair of options was presented the same number of times in the experiment. In this case there may not be much advantage to enforcing the triangle equality.

In comparison, the Shevlin et al. [26] dataset is incomplete, and some pairs of values are presented many more times than others. In this case, there may be an opportunity for our estimator to fill in gaps in the data. Indeed, when we examined the Shevlin et al. [26] dataset we found that the cyclic estimator had significantly lower absolute deviations (medians: Low = 0.72, Medium = 0.60, High = 0.66) than the logistic estimator (medians: Low = 2.73, Medium = 2.51, High = 2.10), for all three value tiers ($p < 10^{-10}$, $p < 10^{-12}$, $p < 10^{-13}$). Thus, the cyclic estimator significantly outperformed the standard logistic-regression approach.

Compared to the HDDM estimator (medians: Low = 0.63, Medium = 0.48, High = 0.72), the cyclic estimator was equivalently good in the Low- and High-value tiers ($p = 0.67$, $p = 0.92$) but significantly worse in the Medium-value tier ($p = 0.0002$). The HDDM estimator significantly outperformed the logistic estimator in all cases ($p = 10^{-9}$, $p = 10^{-13}$, $p = 10^{-13}$). Thus, despite using much more data, the HDDM performed no better than our cyclic estimator in most cases.

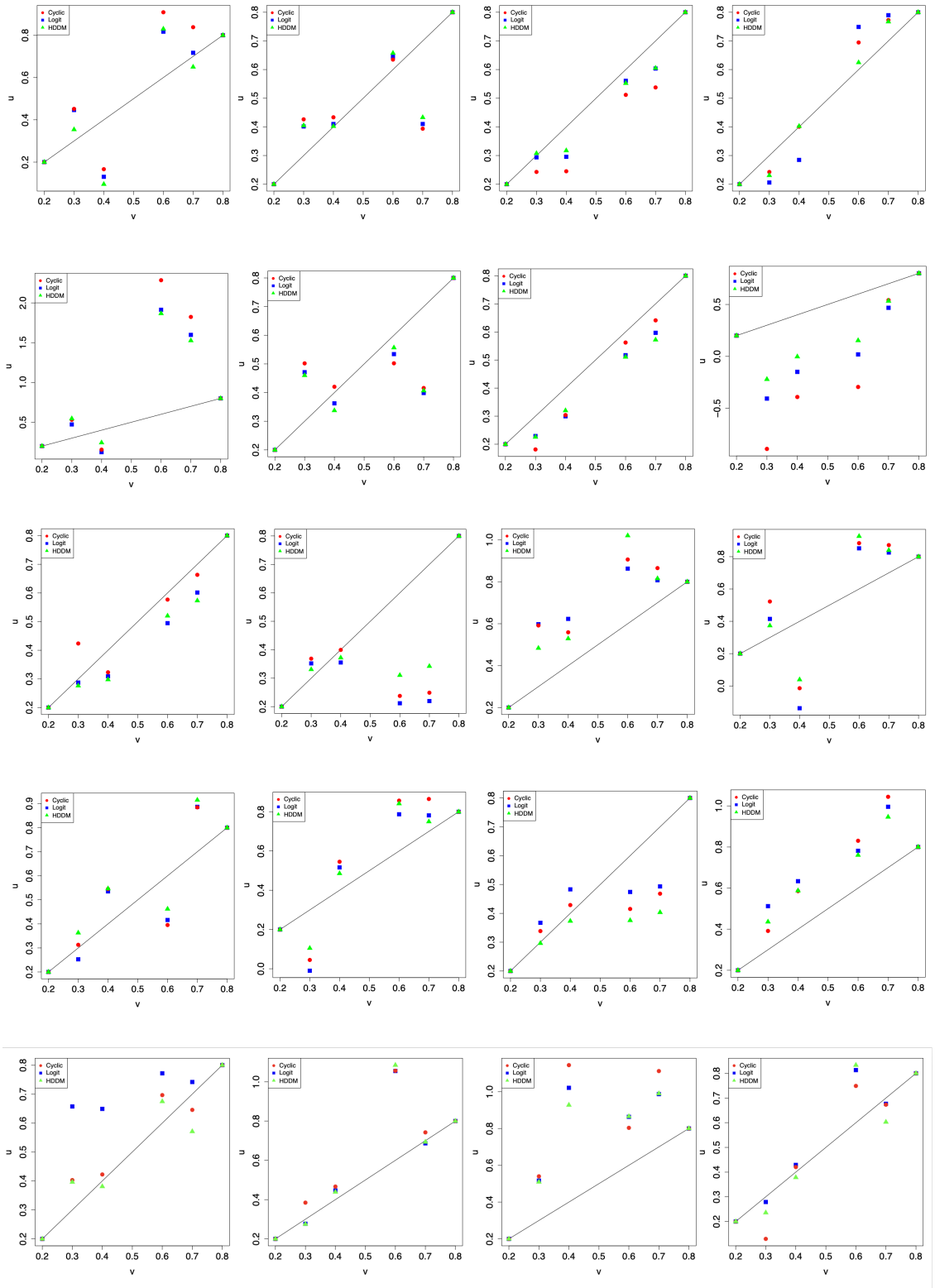

Figure S1: Utility (u) vs. value (v) for each subject in the Cavanagh et al. [25] dataset. These plots display a linear relationship (diagonal black line) as well as the fits from our cyclic estimator, HDDM, and a logistic regression. Because utility is on an arbitrary scale, we forced the lowest and highest utilities to be accurate and then measured the relative locations of the remaining estimates.

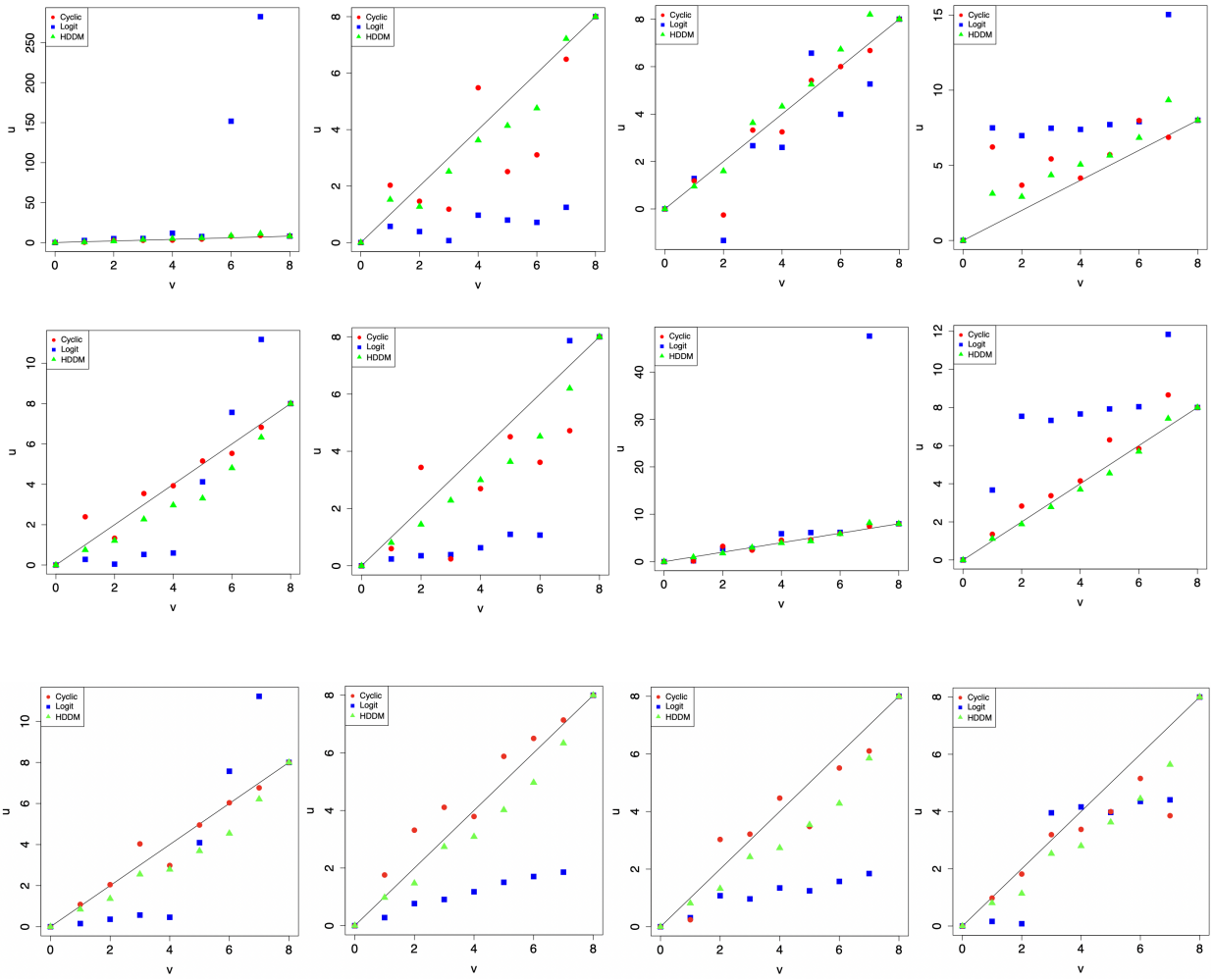

Figure S2: Utility (u) vs. value (v) for randomly selected participants in the Shevlin et al. [26] dataset, four each for the low (top row), medium (middle row), and high (bottom row) value tiers. These plots display a linear relationship (diagonal black line) as well as the fits from our cyclic estimator, HDDM, and a logistic regression. Because utility is on an arbitrary scale, we forced the lowest and highest utilities to be accurate and then measured the relative locations of the remaining estimates.

5.3.2 Simulated data

Here we present results of parameter recovery exercises, carried out to ensure that our cyclic estimator can recover parameters accurately. Unlike with the empirical data, here we know the ground truth.

We simulated datasets using three different mappings from value to utility, namely $U(v) = v^x$ where x is either 0.5, 1, or 2. For v we used all the integers from 1 to 10, yielding 45 unique pairs. For the other parameters like boundary separation (λ) and non-decision time, we used values estimated from similar value-based studies [3]. We produced two versions of each dataset, one with data produced by a single "subject" (i.e., a single set of parameters) and another with data produced by ten different "subjects" (with each parameter drawn from a Normal distribution; mean $\lambda = 71$, mean non-decision time = 350 ms). In total, we simulated 6 datasets.

Our primary concern is whether the model recovers the utility functions accurately. In Figure S3 we see that indeed the cyclic estimator accurately recovers the true utilities. For comparison we also show the fits from HDDM and a logistic regression.

The other parameter that we estimate is λ, the boundary separation. The datasets were simulated with a boundary separation of $\lambda = 71$. The recovered λ for the six datasets were: 80, 77, 80, 74, 78, 79 for the linear (1, 10 subjects), quadratic (1, 10 subjects), and square root (1, 10 subjects) datasets respectively. As expected, our estimator slightly overestimates the boundary separation since it does not account for the non-decision time contribution to the RT.

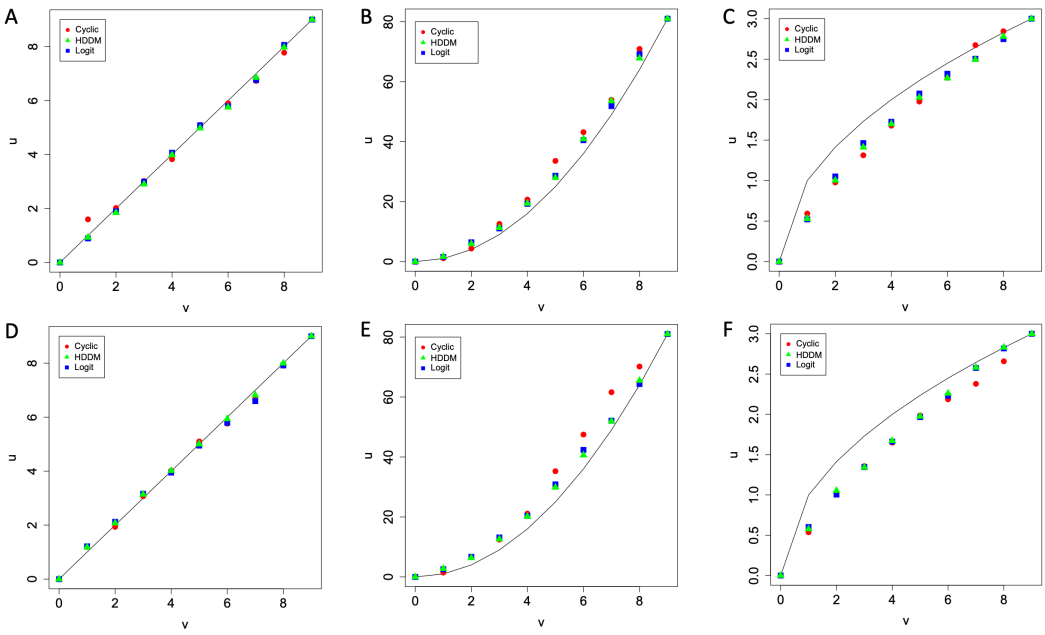

Figure S3: Utility (u) vs. true value (v) for the simulated data, using (A,D) linear utility, (B,E) squared utility, and (C,F) square root utility. The top row (A-C) displays simulated datasets with a single set of parameters, while the bottom row (D-F) displays simulated datasets with 10 sets of parameters (i.e., 10 simulated subjects). These plots display the true relationship (black line) as well as the fits from our cyclic estimator, HDDM, and a logistic regression. Because utility is on an arbitrary scale, we force the lowest and highest utilities to be accurate and then measure the relative locations of the remaining estimates.

Additionally, we sought to confirm our results in the previous section that the cyclic estimator outperforms a logistic regression estimator for subject-level utility estimates. To do so, we simulated one additional dataset with the square-root function from value to utility. For this exercise we used the same parameter distributions as before, but we simulated 100 "subjects", each with 0-4 observations per pair of items in the set ($v = [1, 10]$). The average "subject" had 90 trials. As before, we compared our cyclic estimator to the logistic regression estimator by calculating the mean absolute deviation from the true values. Our cyclic estimator significantly outperformed the logistic regression estimator (median error: cyclic = 1.60, logistic = 1.83; $p = 0.04$), using a paired Mann-Whitney-Wilcoxon test. This confirms our intuition that the cyclic estimator can outperform standard logistic regression with imbalanced datasets.

At the same time, both the cyclic and logit estimators were substantially bested by the HDDM estimator (median error: 1.05, $p < 0.001$). The HDDM estimator has several advantages - it uses RT and is informed by HDDM's priors. Our cyclic estimator may outperform HDDM in cases where RT is distorted either because the DDM is not exactly the right model or because RT is measured with a lot of noise. To examine this possibility, we took our 100 simulated subjects, randomly permuted the RTs across trials, and then refit the HDDM (the cyclic and logit estimators are unaffected by the RT permutation). In this case the cyclic estimator did indeed outperform HDDM – the median errors were Logit = 1.83, HDDM = 1.69, Cyclic = 1.60, though the differences between HDDM and the others were not significant (Logit: $p = 0.24$, Cyclic: $p = 0.19$). Interestingly, HDDM still outperformed logit. We suspect that this is because the priors in HDDM prevent the drift-rate estimates from becoming too extreme. In terms of computation time, the cyclic estimator has a huge advantage over HDDM. The HDDM fits for these 100 simulated subjects took 577 minutes. The cyclic estimator took 190 microseconds. That is an improvement in computation time of 8 orders of magnitude.

5.4 Goodness of fit

When fitting DDMs (or other models) to data, it is important to check their absolute goodness of fit. For the DDM, this is typically done with quantile-probability (QP) plots, which compare choice probabilities and RT quantiles for the data and model. Here we present QP plots for both the simulated (Fig. S4) and empirical data (Fig. S5).

It is worth noting that the model provides reasonable fits to the simulated data but struggles more with the empirical data. The DDM consistently underestimates the lowest quantiles, presumably because we did not include a non-decision

time parameter in the fits. Indeed, it would be surprising/troubling if the DDM was able to perfectly match the data in the QP plots without that parameter. In the next section we address the non-decision time issue.

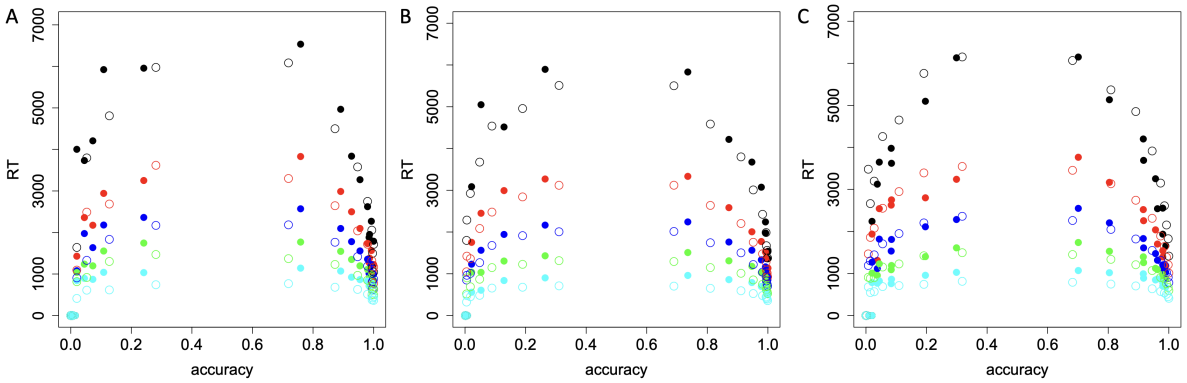

Figure S4: Quantile probability plots for the simulated datasets. These plots show the relationship between RT and accuracy for each condition (value-difference level). Each condition is represented twice, once for correct responses (accuracy: right of 0.5) and once for errors (1–accuracy: left of 0.5). The solid dots denote the data, and the open circles denote the DDM fits. The cyan, green, blue, red, and black symbols denote the 0.1, 0.3, 0.5, 0.7, 0.9 RT quantiles. Data were simulated with (A) linear utility, (B) squared utility, and (C) square-root utility. Points at (0,0) represent conditions where there were fewer than 5 observations.

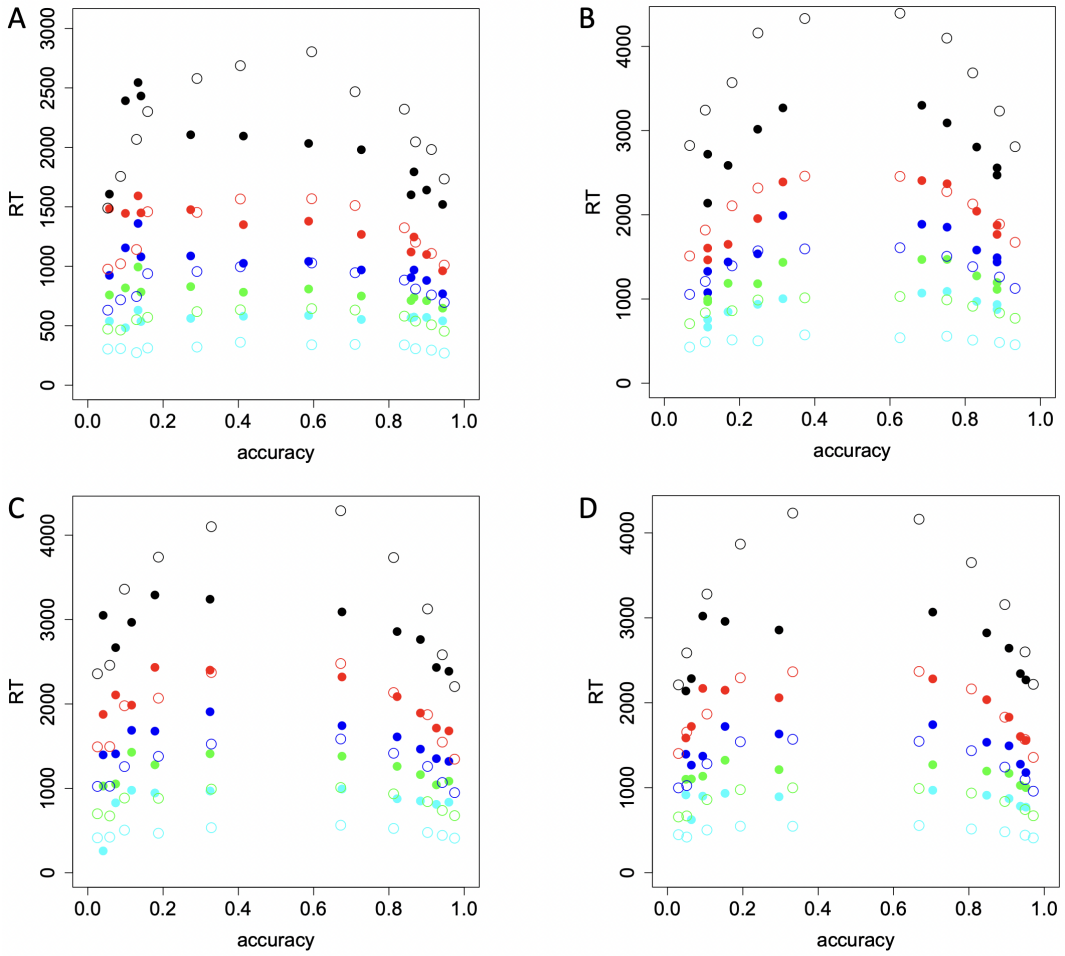

Figure S5: Quantile probability plots for the empirical datasets. These plots show the relationship between RT and accuracy for each condition (value-difference level). Each condition is represented twice, once for correct responses (accuracy: right of 0.5) and once for errors (1–accuracy: left of 0.5). The solid dots denote the data, and the open circles denote the DDM fits. The cyan, green, blue, red, and black symbols denote the 0.1, 0.3, 0.5, 0.7, 0.9 RT quantiles. Data are from the (A) Cavanagh et al. [25] dataset, (B) Low value tier, (C) Medium value tier, and (D) High-value tier of the Shevlin et al. [26] dataset. Points at (0,0) represent conditions where there were fewer than 5 observations.

5.4.1 Non-decision times

Here we ran an additional analysis where we estimated the non-decision time for each empirical dataset (using HDDM; Cavanagh = 260 ms, Shevlin = 228 ms), subtracted it from each RT, and then refit the cyclic estimator on the resulting decision times (DT). Below we present QP plots for the empirical data, fit this way (Fig. S6).

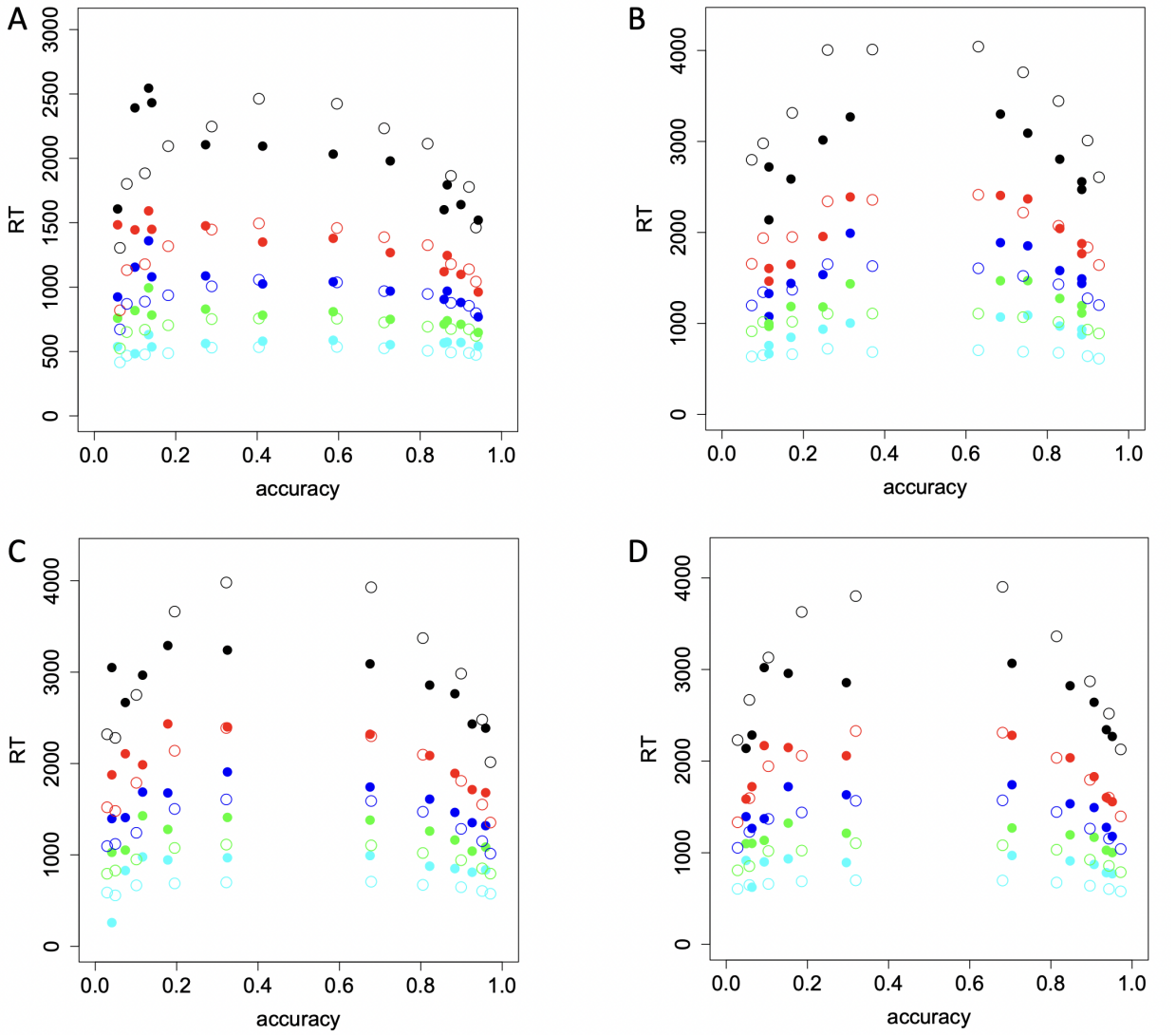

Figure S6: Quantile probability plots for the empirical datasets, accounting for non-decision time. These plots show the relationship between RT and accuracy for each condition (value-difference level). Each condition is represented twice, once for correct responses (accuracy: right of 0.5) and once for errors (1–accuracy: left of 0.5). The solid dots denote the data, and the open circles denote the DDM fits. The cyan, green, blue, red, and black symbols denote the 0.1, 0.3, 0.5, 0.7, 0.9 RT quantiles. Data are from the (A) Cavanagh et al. [25] dataset, (B) Low value tier, (C) Medium value tier, and (D) High-value tier of the Shevlin et al. [26] dataset. Points at (0,0) represent conditions where there were fewer than 5 observations.

5.5 Shevlin et al. [26]: conditioning on group and instruction

In this section we repeat the analysis of the paper by splitting the Shevlin et al. [26] dataset into 6 sub-datasets. The sub-problems are identified by jointly conditioning on the "Third" variable (which can be 1, 2, or 3 depending on whether the corresponding decision problem contains a pair of alternatives coming from the low, medium or high payoff group, respectively), and the "Instr" variable (which can be 0 or 1, depending on whether the subjects know to which group the choice they face comes from).

5.5.1 Third = 1 (low)

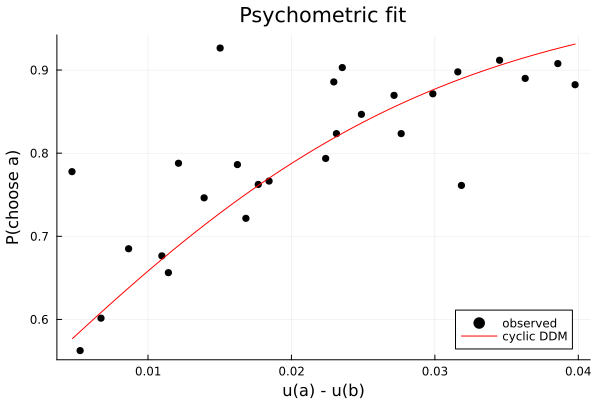

(a) Psychometric fit, Instr = 0

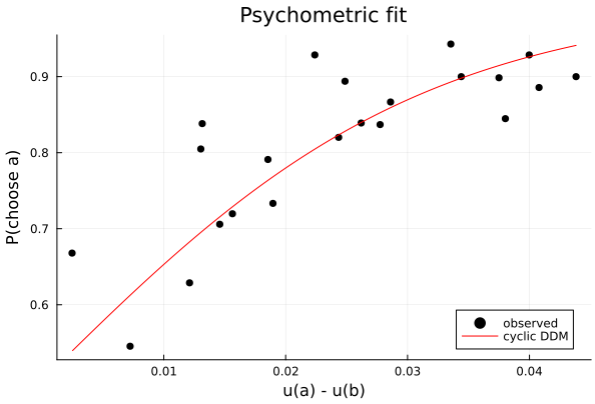

(b) Psychometric fit, Instr = 1

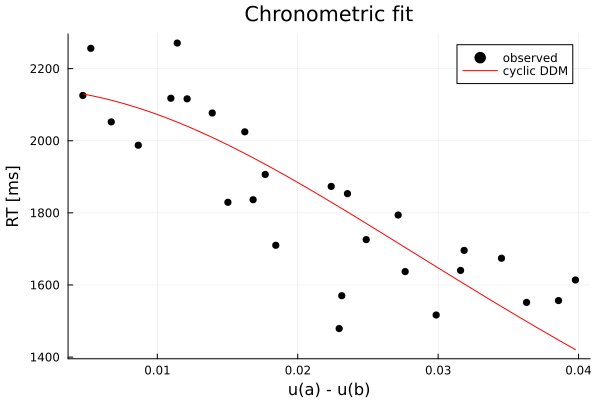

(c) Chronometric fit, Instr = 0

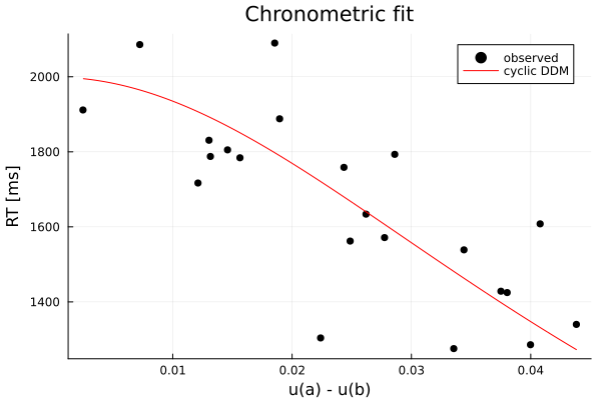

(d) Chronometric fit, Instr = 1

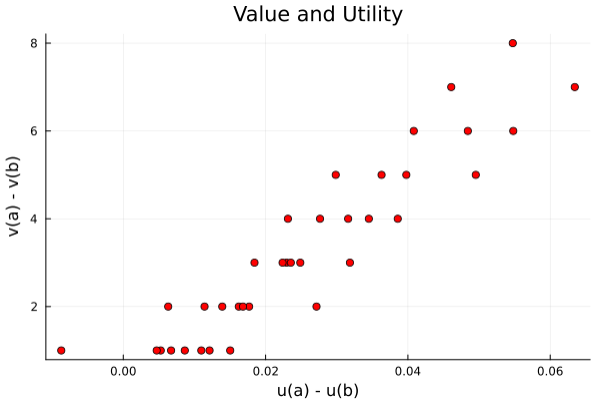

(e) Value vs utility, Instr = 0

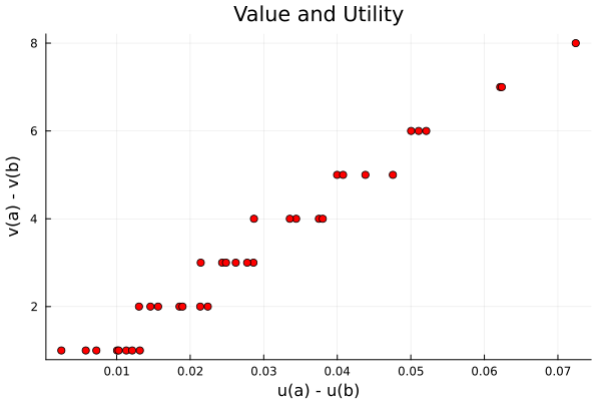

(f) Value vs utility, Instr = 1

Figure S7: Comparison between instructed and non-instructed decision makers for the Group 1.

5.5.2 Third = 2 (medium)

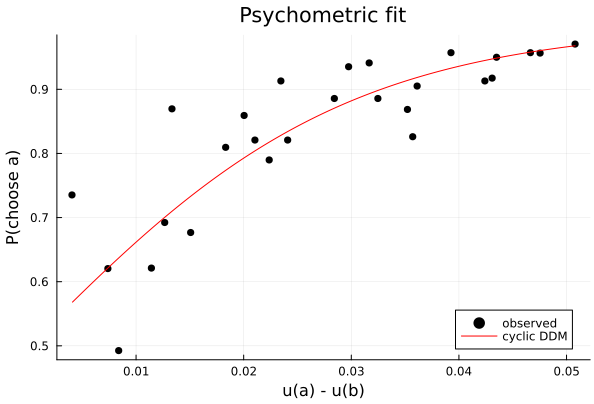

(a) Psychometric fit, Instr = 0

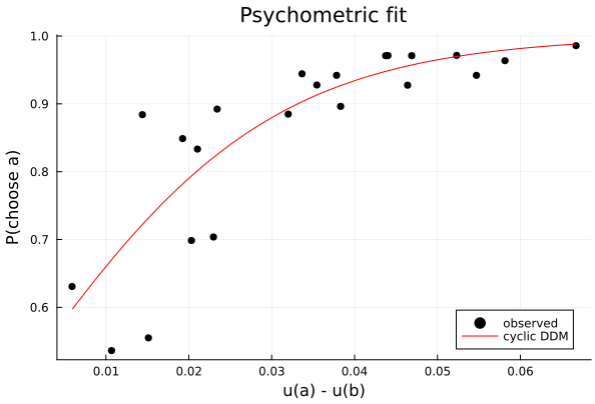

(b) Psychometric fit, Instr = 1

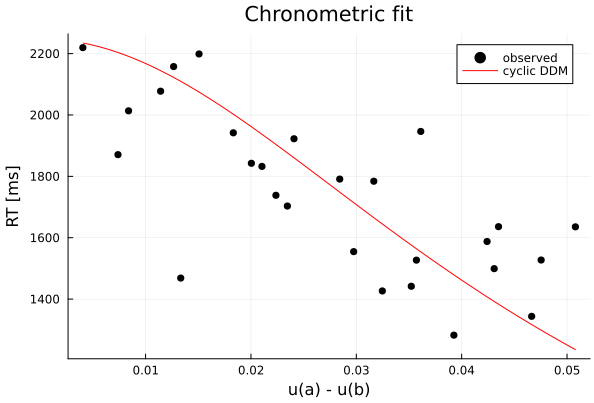

(c) Chronometric fit, Instr = 0

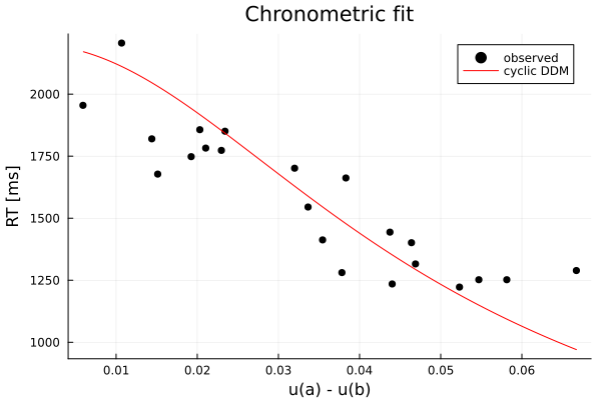

(d) Chronometric fit, Instr = 1

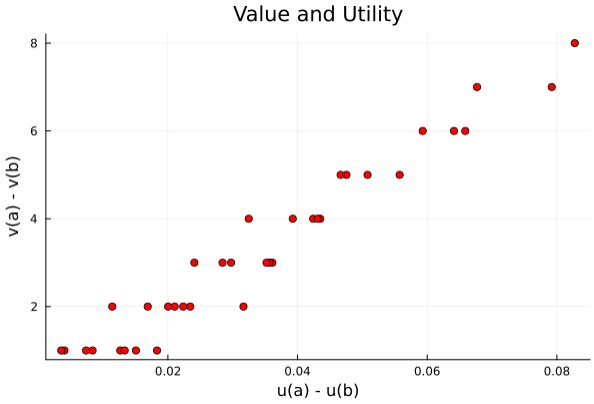

(e) Value vs utility, Instr = 0

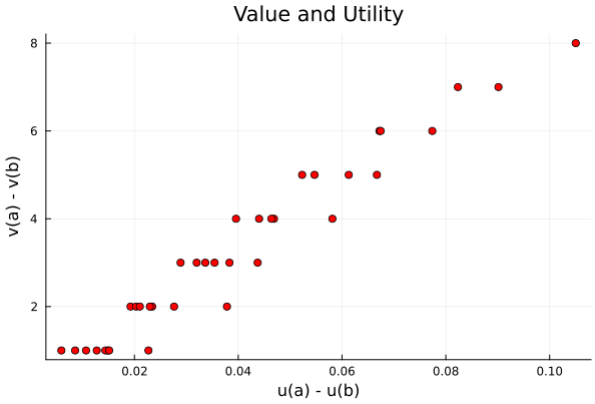

(f) Value vs utility, Instr = 1

Figure S8: Comparison between instructed and non-instructed decision makers for the Group 2.

5.5.3 Third = 3 (high)

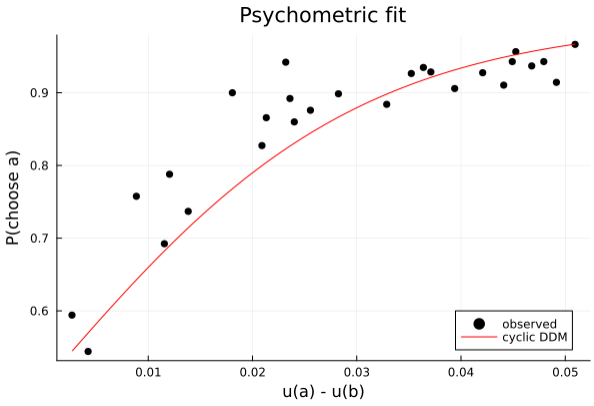

(a) Psychometric fit, Instr = 0

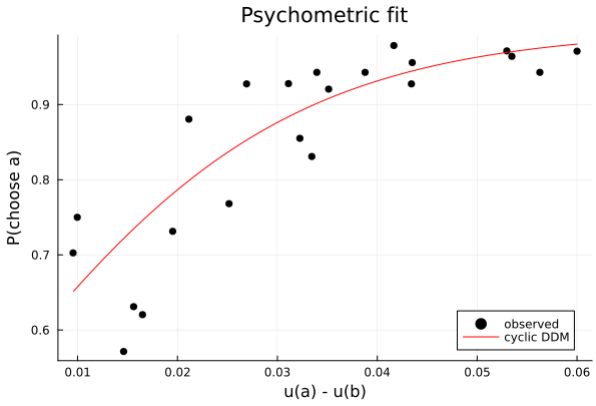

(b) Psychometric fit, Instr = 1

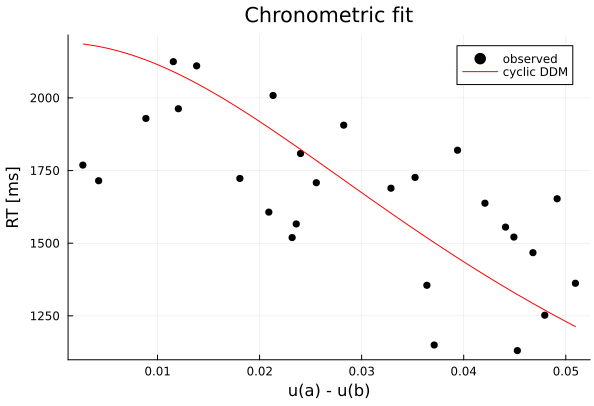

(c) Chronometric fit, Instr = 0

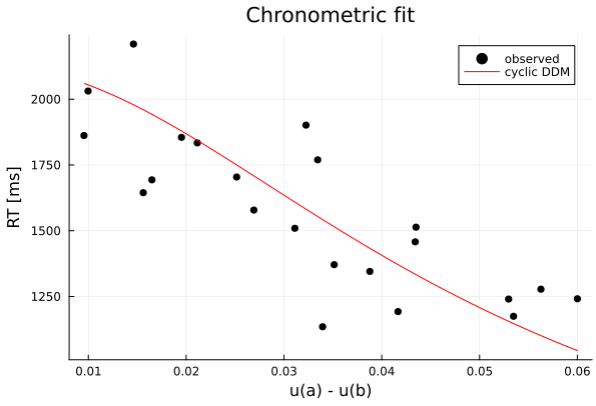

(d) Chronometric fit, Instr = 1

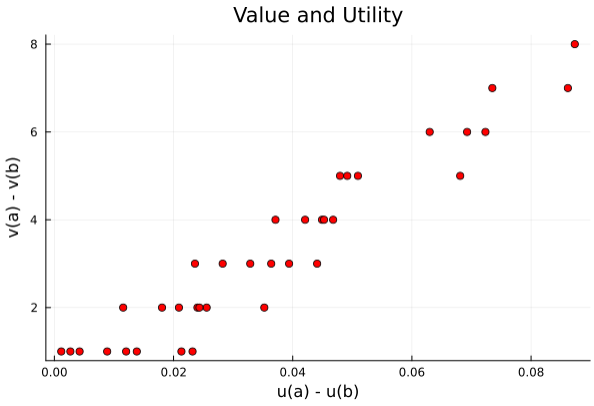

(e) Value vs utility, Instr = 0

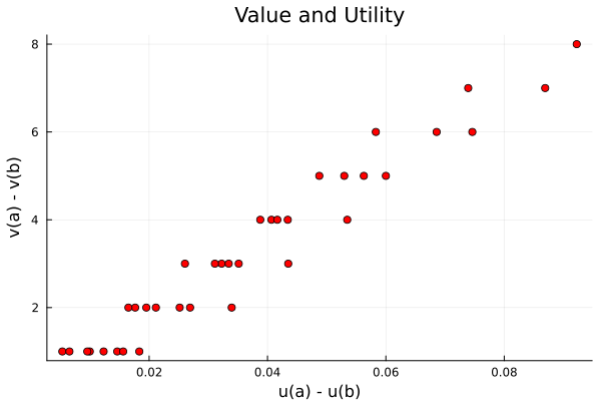

(f) Value vs utility, Instr = 1

Figure S9: Comparison between instructed and non-instructed decision makers for the Group 3.

5.6 Shevlin et al. [26]: no group conditioning, only instructions

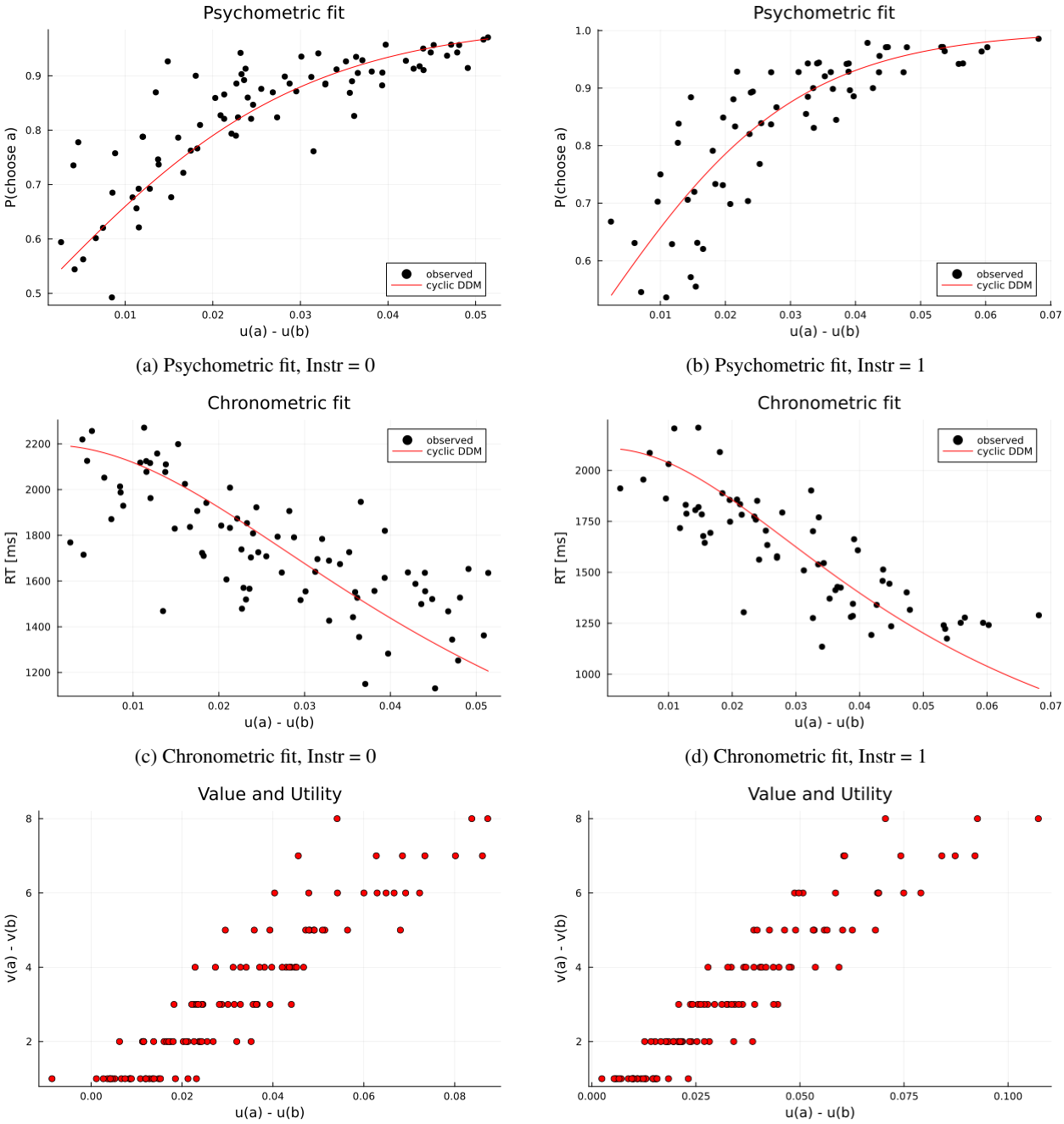

(a) Psychometric fit, Instr = 0

(b) Psychometric fit, Instr = 1

(c) Chronometric fit, Instr = 0

(d) Chronometric fit, Instr = 1

(e) Value vs utility, Instr = 0

(f) Value vs utility, Instr = 1

Figure S10: Comparison between instructed and non-instructed decision makers for the whole dataset.

5.7 Cavanagh et al. [25]: whole vs. no win-win dataset

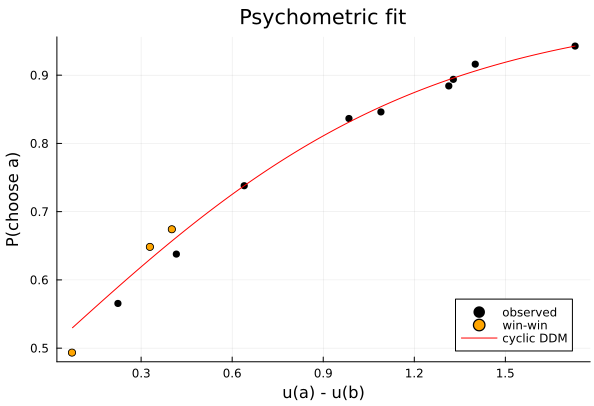

(a) Psychometric fit, whole dataset

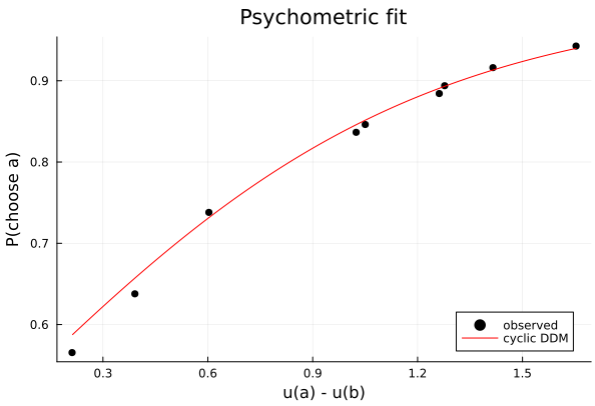

(b) Psychometric fit, no win-win outliers

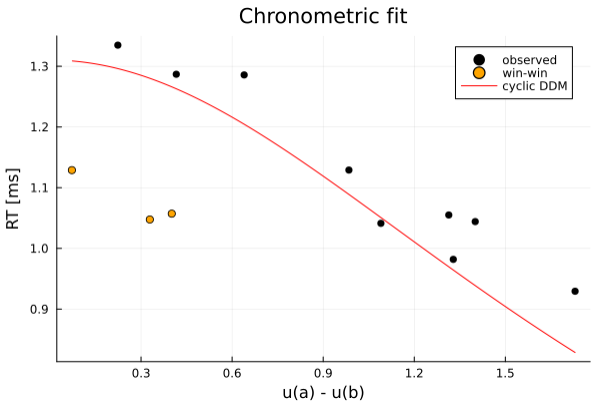

(c) Chronometric fit, whole dataset

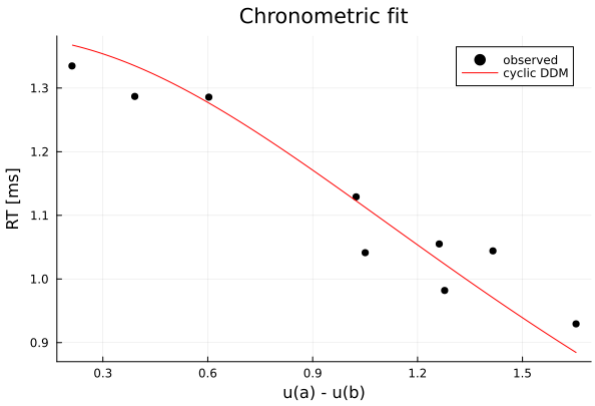

(d) Chronometric fit, no win-win outliers

Figure S11: Comparison between whole and no win-win version of Cavanagh dataset.

REFERENCES AND NOTES

1. M. N. Shadlen, D. Shohamy, Decision making and sequential sampling from memory. *Neuron* **90**, 927–939 (2016).
2. J. R. Busemeyer, S. Gluth, J. Rieskamp, B. M. Turner, Cognitive and neural bases of multi-attribute, multi-alternative, value-based decisions. *Trends Cogn. Sci.* **23**, 251–263 (2019).
3. I. Krajbich, C. Armel, A. Rangel, Visual fixations and the computation and comparison of value in simple choice. *Nat. Neurosci.* **13**, 1292–1298 (2010).
4. R. Ratcliff, A theory of memory retrieval. *Psychol. Rev.* **85**, 59–108 (1978).
5. R. Ratcliff, P. L. Smith, S. D. Brown, G. McKoon, Diffusion decision model: Current issues and history. *Trends Cogn. Sci.* **20**, 260–281 (2016).
6. M. Milosavljevic, J. Malmaud, A. Huth, C. Koch, A. Rangel, The drift diffusion model can account for the accuracy and reaction time of value-based choices under high and low time pressure. *Judgm. Decis. Mak.* **5**, 437–449 (2010).
7. G. Fisher, An attentional drift diffusion model over binary-attribute choice. *Cognition* **168**, 34–45 (2017).
8. J. A. Clithero, Improving out-of-sample predictions using response times and a model of the decision process. *J. Econ. Behav. Organ.* **148**, 344–375 (2018).
9. P. Sepulveda, M. Usher, N. Davies, A. A. Benson, P. Ortoleva, B. De Martino, Visual attention modulates the integration of goal-relevant evidence and not value. *eLife* **9**, e60705 (2020).
10. K. X. Chiong, M. Shum, R. Webb, R. Chen, Combining choice and response time data: A drift-diffusion model of mobile advertisements. *Manage. Sci.* 10.1287/mnsc.2023.4738, (2023).
11. M. Glickman, O. Sharoni, D. J. Levy, E. Niebur, V. Stuphorn, M. Usher, The formation of preference in risky choice. *PLOS Comput. Biol.* **15**, e1007201 (2019).
12. V. Zilker, T. Pachur, Nonlinear probability weighting can reflect attentional biases in sequential sampling. *Psychol. Rev.* **129**, 949–975 (2022).
13. W. J. Zhao, A. Diederich, J. S. Trueblood, S. Bhatia, Automatic biases in intertemporal choice. *Psychon. Bull. Rev.* **26**, 661–668 (2019).
14. J. R. Busemeyer, A. Diederich, Survey of decision field theory. *Math. Soc. Sci.* **43**, 345–370 (2002).
15. A. Konovalov, I. Krajbich, Revealed strength of preference: Inference from response times. *Judgm. Decis. Mak.* **14**, 381–394 (2019).

16. F. Sheng, A. Ramakrishnan, D. Seok, W. J. Zhao, S. Thelaus, P. Cen, M. L. Platt, Decomposing loss aversion from gaze allocation and pupil dilation. *Proc. Natl. Acad. Sci. U.S.A.* **117**, 11356–11363 (2020).
17. J. Dai, J. R. Busemeyer, A probabilistic, dynamic, and attribute-wise model of intertemporal choice. *J. Exp. Psychol. Gen.* **143**, 1489–1514 (2014).
18. D. R. Amasino, N. J. Sullivan, R. E. Kranton, S. A. Huettel, Amount and time exert independent influences on intertemporal choice. *Nat. Hum. Behav.* **3**, 383–392 (2019).
19. I. Krajbich, T. Hare, B. Bartling, Y. Morishima, E. Fehr, A common mechanism underlying food choice and social decisions. *PLOS Comput. Biol.* **11**, e1004371 (2015).
20. C. A. Hutcherson, B. Bushong, A. Rangel, A neurocomputational model of altruistic choice and its implications. *Neuron* **87**, 451–462 (2015).
21. M. Abdellaoui, Parameter-free elicitation of utility and probability weighting functions. *Manage. Sci.* **46**, 1497–1512 (2000).
22. R. Ratcliff, P. L. Smith, A comparison of sequential sampling models for two-choice reaction time. *Psychol. Rev.* **111**, 333–367 (2004).
23. R. Ratcliff, G. McKoon, Modeling numerosity representation with an integrated diffusion model. *Psychol. Rev.* **125**, 183–217 (2018).
24. C. Baldassi, S. Cerreia-Vioglio, F. Maccheroni, M. Marinacci, M. Pirazzini, A behavioral characterization of the drift diffusion model and its multialternative extension for choice under time pressure. *Manage. Sci.* **66**, 5075–5093 (2020).
25. J. F. Cavanagh, T. V. Wiecki, A. Kochar, M. J. Frank, Eye tracking and pupillometry are indicators of dissociable latent decision processes. *J. Exp. Psychol. Gen.* **143**, 1476–1488 (2014).
26. B. R. K. Shevlin, S. M. Smith, J. Hausfeld, I. Krajbich, High-value decisions are fast and accurate, inconsistent with diminishing value sensitivity. *Proc. Natl. Acad. Sci.* **119**, e2101508119 (2022).
27. O. Bartra, J. T. McGuire, J. W. Kable, The valuation system: A coordinate-based meta-analysis of bold fmri experiments examining neural correlates of subjective value. *Neuroimage* **76**, 412–427 (2013).
28. J. A. Clithero, A. Rangel, Informatic parcellation of the network involved in the computation of subjective value. *Soc. Cogn. Affect. Neurosci.* **9**, 1289–1302 (2014).
29. S. M. Smith, I. Krajbich, Mental representations distinguish value-based decisions from perceptual decisions. *Psychon. Bull. Rev.*, **28**, 1413–1422 (2021).

30. B. Oksendal, *Stochastic Differential Equations: An Introduction with Applications* (Springer Science & Business Media, 2013).
31. L. Wasserman, *All of Nonparametric Statistics* (Springer Science & Business Media, 2006).
32. R. Webb, The (neural) dynamics of stochastic choice. *Manage. Sci.* **65**, 230–255 (2019).
33. M. J. Frank, Hold your horses: A dynamic computational role for the subthalamic nucleus in decision making. *Neural Netw.* **19**, 1120–1136 (2006).
34. T. V. Wiecki, M. J. Frank, A computational model of inhibitory control in frontal cortex and basal ganglia. *Psychol. Rev.* **120**, 329–355 (2013).
35. R. Polanía, I. Krajbich, M. Grueschow, C. C. Ruff, Neural oscillations and synchronization differentially support evidence accumulation in perceptual and value-based decision making. *Neuron* **82**, 709–720 (2014).
36. J. Hascher, N. Desai, I. Krajbich, Incentivized and non-incentivized liking ratings outperform willingness-to-pay in predicting choice. *Judgm. Decis. Mak.* **16**, 1464–1484 (2021).
37. S. Cerreia-Vioglio, F. Maccheroni, M. Marinacci, A. Rustichini, Multinomial logit processes and preference discovery: Inside and outside the black box. *Rev. Econ. Stud.* **90**, 1155–1194 (2023).
38. D. Kahneman, A. Tversky, On the interpretation of intuitive probability: A reply to jonathan cohen. *Cognition* **7**, 409–411 (1979).
39. R. Hertwig, G. Barron, E. U. Weber, I. Erev, Decisions from experience and the effect of rare events in risky choice. *Psychol. Sci.* **15**, 534–539 (2004).
40. M. J. Frank, L. C. Seeberger, R. C. O'reilly, By carrot or by stick: Cognitive reinforcement learning in parkinsonism. *Science* **306**, 1940–1943 (2004).
41. A. Pirrone, H. Azab, B. Y. Hayden, T. Stafford, J. A. R. Marshall, Evidence for the speed–value trade-off: Human and monkey decision making is magnitude sensitive. *Decision* **5**, 129–142 (2018).
42. B. R. K. Shevlin, I. Krajbich, Attention as a source of variability in decision-making: Accounting for overall-value effects with diffusion models. *J. Math. Psychol.* **105**, 102594 (2021).
43. R. Ratcliff, M. J. Frank, Reinforcement-based decision making in corticostriatal circuits: Mutual constraints by neurocomputational and diffusion models. *Neural Comput.* **24**, 1186–1229 (2012).
44. A. Wald, Sequential tests of statistical hypotheses. *Ann. Math. Stat.* **16**, 117–186 (1945).
45. M. Woodford, Stochastic choice: An optimizing neuroeconomic model. *Am. Econ. Rev.* **104**, 495–500 (2014).
46. F. Echenique, K. Saito, Response time and utility. *J. Econ. Behav. Organ.* **139**, 49–59 (2017).

47. D. Fudenberg, P. Strack, T. Strzalecki, Speed, accuracy, and the optimal timing of choices. *Am. Econ. Rev.* **108**, 3651–3684 (2018).
48. S. Tajima, J. Drugowitsch, A. Pouget. Optimal policy for value-based decision-making. *Nat. Commun.* **7**, 12400 (2016).
49. C. Alós-Ferrer, E. Fehr, N. Netzer, Time will tell: Recovering preferences when choices are noisy. *J. Political Econ.* **129**, 1828–1877 (2021).
50. R. Bhui, Testing optimal timing in value-linked decision making. *Comput. Brain Behav.* **2**, 85–94 (2019).
51. C. Frydman, G. Nave, Extrapolative beliefs in perceptual and economic decisions: Evidence of a common mechanism. *Manage. Sci.* **63**, 2340–2352 (2017).
52. C. Frydman, I. Krajbich, Using response times to infer others' private information: an application to information cascades. *Manage. Sci.* **68**, 2970–2986 (2022).
53. C. N. White, R. A. Poldrack, Decomposing bias in different types of simple decisions. *J. Exp. Psychol. Learn. Mem. Cogn.* **40**, 385–398 (2014).
54. N. Desai, I. Krajbich, Decomposing preferences into predispositions and evaluations. *J. Exp. Psychol. Gen.* **151**, 1883–1903 (2022).
55. R. Bogacz, E.-J. Wagenmakers, B. U. Forstmann, S. Nieuwenhuis, The neural basis of the speed–accuracy tradeoff. *Trends Neurosci.* **33**, 10–16 (2010).
56. U. Basten, G. Biele, H. R. Heekeren, C. J. Fiebach, How the brain integrates costs and benefits during decision making. *Proc. Natl. Acad. Sci. U.S.A.* **107**, 21767–21772 (2010).
57. T. A. Hare, W. Schultz, C. F. Camerer, J. P. O'Doherty, A. Rangel, Transformation of stimulus value signals into motor commands during simple choice. *Proc. Natl. Acad. Sci. U.S.A.* **108**, 18120–18125 (2011).
58. S. Gluth, J. Rieskamp, C. Büchel, Deciding when to decide: Time-variant sequential sampling models explain the emergence of value-based decisions in the human brain. *J. Neurosci.* **32**, 10686–10698 (2012).
59. B. M. Turner, L. Van Maanen, B. U. Forstmann, Informing cognitive abstractions through neuroimaging: The neural drift diffusion model. *Psychol. Rev.* **122**, 312–336 (2015).
60. M. A. Pisauro, E. Fouragnan, C. Retzler, M. G. Philiastides, Neural correlates of evidence accumulation during value-based decisions revealed via simultaneous EEG-fMRI. *Nat. Commun.* **8**, 15808 (2017).

61. S. Gluth, N. Meiran, Leave-one-trial-out, loto, a general approach to link single-trial parameters of cognitive models to neural data. *eLife*, **8**, e42607 (2019).
62. J. Aczél, *Lectures on Functional Equations and Their Applications* (Academic Press, 1966).
63. E.-J. Wagenmakers, H. L. J. Van Der Maas, R. P. P. P. Grasman, An ez-diffusion model for response time and accuracy. *Psychon. Bull. Rev.* **14**, 3–22 (2007).
64. J. M. Cattell, The time of perception as a measure of differences in intensity. *Philos. Stud.* **19**, 63–68 (1902).